*Euro. Jnl of Applied Mathematics* (2019), *vol.* 30, *pp.* 529–556.  
doi:10.1017/S095679251800027X

# Macroscopic models for calcium carbonate corrosion due to sulfation. Variation of diffusion and volume expansion

CHRISTOS V. NIKOLOPOULOS

*Department of Mathematics, University of the Aegean, Karlovasi, 83200 Samos, Greece*
*email: cnikolo@aegean.gr*

(*Received 26 January 2017; revised 7 May 2018; accepted 9 May 2018; first published online 6 June 2018*)

The subject of the present paper is the derivation and analysis of mathematical models for the formation of a mushy region during calcium carbonate corrosion. More specifically there is emphasis on the variation of the overall diffusion resulting from the changing shape of a single pore due to corrosion process and on the resulting volume expansion of the material as the outcome of the transformation of calcium carbonate to gypsum. These models are derived by averaging, with the use of the multiple scales method applied on microscopic moving-boundary problems. The latter problems describe the transformation of calcium carbonate into gypsum in the microscopic scale. The derived macroscopic models are solved numerically with the use of an implicit in time, finite element method. The results of the simulations for various microstructure geometries in the micro-scale and a discussion are also presented.

**Key words:** Sulfation, concrete corrosion, monument corrosion, moving boundary problems, perturbation methods

## 1 Introduction

The reaction of hydrogen sulphide or sulphur dioxide with calcium carbonate leads to the creation of gypsum. These reactions are the basic cause for corrosions such as sewer pipes corrosion [5], monument's corrosion [8], building decay (failures in building fabric caused by corrosion). Mathematical modelling of such a process is useful in order to predict the evolution of the phenomenon, as well as its dependence on the physical quantities effecting it. In some cases this can also allow us to choose an optimal strategy to restore or preserve the construction or the monument.

In this framework mathematical models have been developed to describe the sewer pipes corrosion. This was initiated in [5] where a model of Stefan type was presented and analysed. This model was further analysed in later papers as in [6,9,10,20]. In the case of monument corrosion, again a model of Stefan type was presented in [7,8]. Additionally, a hydrodynamic model for sulfation of calcium carbonate stones in the form of a reaction diffusion system was presented and analysed extensively in [1–3,12,13].

In the above models a distinct interface separates the corroded and uncorroded parts of the material. An additional factor that the modelling of these phenomena has to take into account is that concrete, cement based constructions, as well as a lot of monuments, for example, made of limestone, are porous materials. Then, the reaction causing the

corrosion takes place inside the pores of the material. This creates a zone in which the calcite surrounding the pores is partly corroded and transformed to gypsum, that is we have a kind of mushy region. The latter region is formed in the area near the macroscopic interface that separates the uncorroded region from the partly corroded one (see Figure 2, point C). Such a model, motivated by the works [17,18] describing the solid–liquid phase change, was initially introduced in [22] and extended in [23] for the case of sewer pipes corrosion. Also for the case of monument corrosion a very similar model was developed in [24].

In the previous models the problem is stated in the microstructure as a typical phase change problem with a moving boundary. Then, applying the process of homogenization, macroscopic equations were derived for the macroscopic scale that is the bulk of the material. In this work we present an extension of such a modelling approach. The first additional aspect that it is addressed here is the volume expansion. Transformation of calcite to gypsum causes volume expansion due to the lower density of gypsum compared to the calcite. In the previous relevant works this was neglected for simplification. Another additional aspect addressed here is the fact that it is assumed there is no diffusion throughout the calcite skeleton. As it will be apparent later in the analysis of the present model, this consideration will lead to the variation of the diffusion coefficient of the macroscopic equation, which is subject to the shape and the area occupied by the calcite inside a pore. The modelling approach in the previous works [22–24] is valid if on the contrary it is assumed that we have diffusion everywhere inside the material, even inside the calcite skeleton due to pores of minor size (reaction takes place only into larger pores). The latter assumption is not a very realistic one but it simplified the analysis and especially the numerical treatment of the problem.

In order to derive a model for the process, initially we need to make some assumptions about the geometry and the microstructure of the material. A two-dimensional approach is used here. Note that the derivation and analysis is valid for all dimensions, with minor modifications, but the specific application has only been presented in two dimensions to avoid at present numerical complications arising in three dimensions. The bulk of the material is assumed to consist of microscopic identical square cells each one corresponding to a pore of the material. The detailed description of that is presented in Section 2. Additionally, the equations describing the diffusion inside the pores together with the equations of the moving boundary (outer boundary of the cell and of the shrinking calcite core) are presented. Next in Section 3, the homogenization (averaging) method is applied to derive the macroscopic equations. In Section 4, it is examined how this set of equations is modified and tackled, via appropriate transformations when this is needed, in order to treat numerically the problem. Finally, in Section 5 some numerical simulations are presented together with the adjustment of the model in the sewer pipes corrosion process, as well as in the case of the monument corrosion.

## 2 Presentation of the model

*Description of an idealized porous material.* Concrete or limestone are porous materials that consist basically of calcium carbonate. Thus, in general, we can think of a material under study being a porous one with its skeleton (the solid part of it) consisting of calcium

https://doi.org/10.1017/S095679251800027X Published online by Cambridge University Press

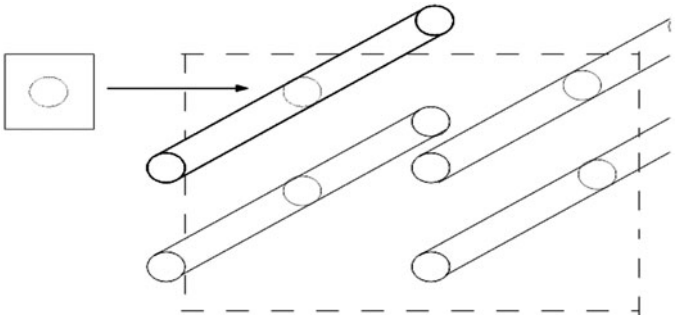

FIGURE 1. Schematic representation of a plane cross-secting parallel bars of a calcium carbonate skeleton. A square on that plane containing the cross section, a circle in this case, centred in it can be considered as one cell in our model.

carbonate. This material under certain cases may be corroded due to sulfate or sulfur dioxide.

We briefly present the basic assumptions used to describe the material which will enable us to derive a model for its corrosion. Actually, this is basically the same setting as it is described also in [22–24].

We assume that the bulk of the material under study, consists of uniform cells and that a subdomain of these cells is filled with calcium carbonate, while the rest of it is void. A natural and fairly simple choice is to assume that these cells are of square form. This will give a two-dimensional geometrical description of the microstructure in which we will focus in this work.

This geometrical approach can be justified if we consider inside the material, a calcite skeleton consisting of long narrow cylindrical bars that are equispaced and parallel. Then, we may think of a plane intersecting these cylinders transversely and obtain a sequence of equispaced circular segments corresponding to the calcite parts, while the rest of the plane corresponds to a net of voids (see Figure 1). Next, taking advantage of this symmetrical setting, we consider square cells filling the plane with each one of them containing a calcite segment centred in it while the rest is void (Figure 2(a)). We may as well assume that the skeleton bars have different forms, such as parallelipipedonal giving a square or parallelogram calcite core or elliptic cylinder giving elliptical calcite core.

Note that our analysis can be carried out similarly if we assume that we have cells that are line segments and have a one-dimensional geometry [22] or alternatively if we consider cubical cells and three-dimensional geometry [23, 24]. Although in the latter three-dimensional case the numerical complications are increased and such a case will not be studied in the present work.

It is also worth mentioning that this two-dimensional setting for the microstructure can be further generalized if we consider hexagonal cells or any other polygonal cells filling the plane. Moreover, in each of the above cases we may have an inverted setting, that is, we can take the core of the cells being the void and the rest of the cell filled with calcite. Therefore, we can finally have geometry-dependent variations of the model but with no essential difference in its basic characteristics and so these considerations will not be studied further here.

Given the above setting about the two-dimensional micro-scale geometry, we may assume, furthermore, that in a local coordinate system a single cell can be defined to occupy initially the square $[-1, 1] \times [-1, 1]$. Additionally the calcite core inside the cell can be taken to be of symmetrical shape and centred inside the cell. The latter assumption simplifies the analysis that follows but it can be easily dropped without significant changes.

*The reactions causing the corrosion.* A material consisting of calcite may be corroded due to the penetration of sulfide or sulfur dioxide inside its pores in the presence of water, causing a reaction which transforms calcite into gypsum.

We will refer to two basic and quite similar reaction processes as follows:

The corrosion of concrete by sulfation is the first process. The basic reaction describing the fact that $H_2SO_4$ reacts with calcite $CaCO_3$ forming gypsum $CaSO_4 \cdot 2H_2O$ and causing concrete corrosion is the following:

$$2H_2O + H^+ + SO_4^{2-} + CaCO_3 \xrightarrow{k} CaSO_4 \cdot 2H_2O + HCO_3^-. \tag{2.1}$$

This is the case in the sewer pipes corrosion, see [5].

In the second case, monument corrosion, we may have penetration of sulfur dioxide inside the pores resulting in a similar reaction, see [7, 8]. The basic reaction in this case describing the fact that $SO_2$ reacts with calcium carbonate $CaCO_3$ forming gypsum $CaSO_4 \cdot 2H_2O$ and causing the corrosion of the monument, is the following:

$$CaCO_3 + SO_2 + \frac{1}{2}O_2 + 2H_2O \xrightarrow{k} CaSO_4 \cdot 2H_2O + CO_2. \tag{2.2}$$

The model for gypsum formation that is derived in [22–24] and extended here allows gypsum and concrete to coexist at some volume element. This element may be specified as one cell as those already described, and having its length side of order similar to the radius of a cross-section of a typical pore. Such a model with minor modifications can account for both the aforementioned reactions.

In the first reaction (concrete corrosion) we have that inside the air and water, $H_2S$ is contained and under a chemical reaction in the water film and this is transformed to $H_2SO_4$. Next, we assume that through the concrete and due to its porosity and the cracks existing in it, there is diffusion (dispersion) of $SO_4^{2-}$, which then reacts with the concrete, that is, the calcite, forming gypsum. The reaction takes place initially at the cracks' inner surface surrounding the pure solid calcite. Due to the reaction gypsum is formed, having larger porosity than that of the concrete, and thus new cracks are formed. Then, diffusion takes place in the gypsum – void, due to cracks, area.

Moreover, due to the fact that the porosity of the gypsum is larger than that of the calcite, we have expansion of the cell volume and hence of the overall volume of the material. The latter is a significant deviation compared with the modelling approach adopted in [22–24]. In addition, another important difference is that we do not allow any kind of diffusion inside the area occupied by the calcite core. Thus, the shape of the calcite will affect, as it will be apparent later, the diffusion behaviour.

The same setting – idealization of the corrosion process – is also assumed for the case that we have limestone or calcium carbonate stone corroded by sulfur dioxide.

Finally, an additional and important assumption that we have to make regarding the

https://doi.org/10.1017/S095679251800027X Published online by Cambridge University Press

relevant size of the diffusion and the reaction rate is that the reaction rate at all times is large enough so as to have a distinct reaction front [5, 8]. In the microscopic scale, the shape of the pore, or equivalently the shape of the calcite core, in the cell will affect the diffusion rate. Consequently, we assume that, even at its maximum, diffusion is not large enough to prevent the formation of a reaction front.

## The model equations

In the following in order to simplify the presentation we will derive initially a basic model keeping the important characteristics of the corrosion process. Then, in each case, for example, in sewer pipes corrosion, monument corrosion or another similar process, the additional aspects or equations can be easily added to describe the actual phenomenon. For the above mentioned cases this is done in Section 5.

We assume that the material under study occupies a domain, denoted by $\Omega_M$, and that the pollutant, $SO_4^{2-}$ or $SO_2$ diffuses inside the pores of it. Its dimensionless concentration satisfies the equation

$$\epsilon u_\tau = \Delta u + f, \tag{2.3}$$

where $u$ is the molar concentration of $\mathrm{SO}_4^{2-}$ ( or of $\mathrm{SO}_2$) , $\epsilon$ is a dimensionless parameter (= typical macroscopic length scale squared over diffusion coefficient and typical time scale) and $f$ being a source term modelling the possible production or supply of $\mathrm{SO}_4^{2-}$ (or of $\mathrm{SO}_2$) in the system.

Moreover, $u = u(y, \tau)$ and in general $y \in \Omega_M \subset \mathbb{R}^n$, $n = 1, 2, 3$ depends on the macroscopic geometry of the material under study. Also $\tau$ is the dimensionless time variable.

The chemical reaction is taking place inside the pores of the material and at the outer surface of solid calcium carbonate. This interface will be denoted by $\Gamma_M$. This interface changes with time, due to the reaction and its motion given by the standard kinetic condition expressing the fact that *Speed of the moving Boundary* $\times$ *Calcium Carbonate concentration* $\propto$ *Rate of reaction*. Regarding the rate of reaction, without loss of generality, we may assume that it has the form $R = R(u(y, \tau)) = u(y, \tau)$ as in the case of sewer pipes corrosion [22,23]. This law can be modified accordingly to account for a different reaction as in the case of monument corrosion, see [24]. Any such modification would not change the analysis that follows.

Summarizing the above, we have that at the boundary $\Gamma_M$ the kinetic condition expressing its motion should be

$$\mathsf{V} = R(u), \quad y \in \Gamma_M, \tag{2.4}$$

where $\mathsf{V}$ is the speed of the moving boundary.

Furthermore, the flux of $u$ arriving at the interface is consumed by the chemical reaction transforming calcite into gypsum. Thus, the boundary condition at the interface of the corroded–uncorroded material, given that $\mathsf{V} = R(y, \tau)$, will be

$$\gamma \frac{\partial u}{\partial n} = \mathsf{V}, \quad y \in \Gamma_M, \tag{2.5}$$

https://doi.org/10.1017/S095679251800027X Published online by Cambridge University Press

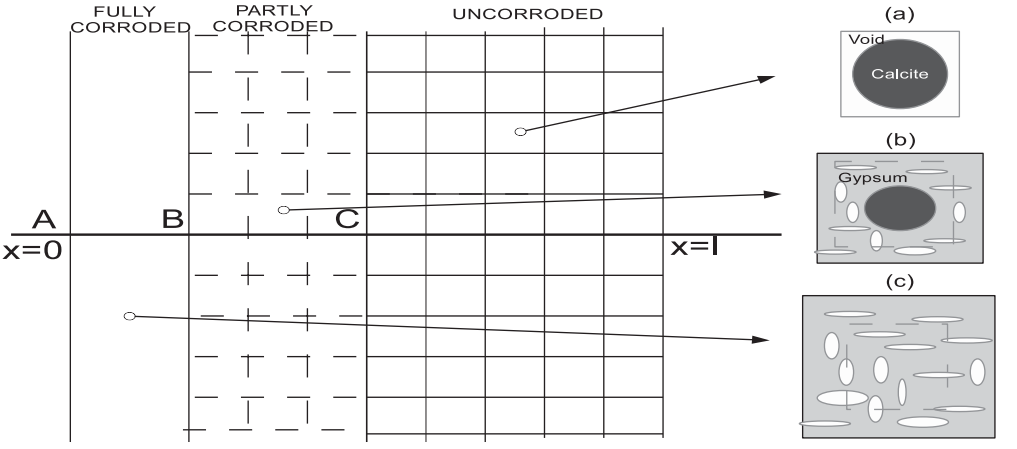


FIGURE 2. Schematic representation of a segment of a calcium carbonate stone under corrosion. In the side cells black colour denotes the area of calcium carbonate and grey colour denotes the gypsum segments while the rest of the cells (white colour) is void space.

where $n$ is the outward normal vector at a point of the moving boundary $\Gamma_M$. This condition may be modified to include also transport of the residual reactant due to the motion of the boundary. In such a case we would have, in dimensionless form, that $\gamma \frac{\partial u}{\partial n} = \mathsf{V} + \mathsf{V}u$. Although the latter at the moment is not included in the model to keep things simple.

Note also that the dimensionless constant $\gamma$ after appropriate scaling can be written as $\gamma = \gamma_u \frac{1}{\delta}$, where $\delta$ is a parameter describing the ratio of the microscopic and macroscopic length scales, defined and discussed in detail later.

These equations apply in the porous net inside the material in $\Omega_M$ but since this is assumed to be consisting of identical two-dimensional cells, we may focus on the behaviour of the model in just one cell. Recall that such a square cell, say $\Omega$, in a local coordinate system initially has the form $\Omega = [-1, 1] \times [-1, 1]$. Also we denote, at all times, its boundary by $\Gamma_e$, $\partial\Omega = \Gamma_e$. This cell initially contains pure calcite occupying a subdomain of it. This subdomain is of symmetrical shape centred inside the cell.

The area occupied by calcite is denoted by $\Omega_c$ and its boundary $\partial\Omega_c = \Gamma_c$ separates it from the void space. Namely, we take the pore, inside the cell, to be specified by the boundaries $\Gamma_e$ and $\Gamma_c$ and its domain, before the corrosion process starts, is $\Omega_v = \Omega \setminus \Omega_c$ (see Figure 2(b)). The area of $\Omega_v$ should be such that $\frac{|\Omega_v|}{|\Omega|} = \phi_c$ for $\phi_c$ being the porosity of the porous material. As corrosion evolves and gypsum is formed, the boundary $\Gamma_c$ now separates pure calcium carbonate from the gypsum and void parts of the rest of the element. We denote the gypsum-void part of the element by $\Omega_g$ and we have $\Omega = \Omega_g \cup \Omega_c$ (see Figure 2(b)). Note that at $t = 0$, $\Omega_g(0) = \Omega_v$. This process continues until the transformation of the calcium carbonate to gypsum is completed and we have $\Omega = \Omega_g$, $\Gamma_c = \emptyset$ (see Figure 2(c)).

The set $\Omega = \Omega(t)$ varies with time due to the expansion caused by the reaction, and this is a significant difference compared with the modelling approach in the works [22–24].

Equation (2.3) applies in $\Omega_g$ and equations (2.4) and (2.5) apply in $\Gamma_c$. We also need

https://doi.org/10.1017/S095679251800027X Published online by Cambridge University Press

boundary conditions for the boundary $\Gamma_e$. Since the material is assumed to be consisting of cells of the same form, we impose periodic conditions. Denoting the four sides of the square cell by $\Gamma_e^i$, $i = 1, \ldots, 4$, with $\Gamma_e = \cup_{i=1}^4 \Gamma_e^i$, we write

$$u_{\Gamma_e^1} = u|_{\Gamma_e^3}, \qquad u_{\Gamma_e^2} = u|_{\Gamma_e^4} \quad y \in \Gamma_e, \tag{2.6a}$$

$$n \cdot \nabla u|_{\Gamma_e^1} = n \cdot \nabla u|_{\Gamma_e^3}, \qquad n \cdot \nabla u|_{\Gamma_e^2} = n \cdot \nabla u|_{\Gamma_e^4} \quad y \in \Gamma_e. \tag{2.6b}$$

Note that these symmetry conditions can be summarized, see [17, 22] to obtain

$$n \cdot \nabla u|_{\partial\Omega} = 0 \quad y \in \Gamma_e.$$

Additionally, the boundary $\Gamma_e$ is expanding. For an area transformed to gypsum, say $A_g$ ($A_g(\tau) = |\Omega_c|(0) - |\Omega_c|(\tau)$), we expect an increase of the total cell area of $\gamma_a A_g$, where $\gamma_a$ is a factor corresponding to the expansion resulting from one unit area of calcium carbonate transformed to gypsum.

We determine $\gamma_a$ so as to account during the reaction, for both the changes in densities and the porosity. For $\rho_c$ and $\rho_g$ being the values of the real [1] (or solid) densities of calcite and gypsum, respectively, we have, before the reaction initiates, that a unit mass of calcite occupies volume $|\Omega_c|(0) = 1/\rho_c$ in a cell of volume $|\Omega|(0)$. Thus, for $\phi_c$ being the porosity of the calcite, we have $\phi_c = \frac{|\Omega|(0) - 1/\rho_c}{|\Omega|(0)}$ and $|\Omega|(0) = \frac{1}{\rho_c(1-\phi_c)}$. At the end of the process, at time, say $T$, we have that by a molar unit of calcite a molar unit of gypsum is created (conservation of mass). Therefore, the transformed mass of gypsum will occupy volume $1/(\rho_g \times \rho_m)$, for $\rho_m = (\rho_{Mc}/\rho_{Mg})$ where $\rho_{Mg}$ and $\rho_{Mc}$ are the molar densities of gypsum and calcite, respectively. Thus, for $\phi_g$ being the porosity of the gypsum, $\phi_g = \frac{|\Omega|(T) - 1/(\rho_g \rho_m)}{|\Omega|(T)}$ or that $|\Omega|(T) = \frac{1}{\rho_g \rho_m (1-\phi_g)}$. In addition, at the same time, we should have $|\Omega|(T) = |\Omega|(0) + \gamma_a |\Omega_c|(0)$. Therefore, we obtain

$$\frac{1}{\rho_g \rho_m (1-\phi_g)} = \frac{1}{\rho_c (1-\phi_c)} + \gamma_a \frac{1}{\rho_c},$$

or

$$\gamma_a = \frac{\rho_c}{\rho_g \rho_m (1-\phi_g)} - \frac{1}{(1-\phi_c)} = \frac{\rho_c(1-\phi_c) - \rho_g \rho_m (1-\phi_g)}{\rho_g \rho_m (1-\phi_c)(1-\phi_g)}.$$

Note also that $\gamma_a > 0$, for $\rho_c > \rho_g$, $\phi_g > \phi_c$, $\rho_m < 1$ since $\frac{\rho_c}{\rho_g} > 1 > \rho_m \frac{1-\phi_g}{1-\phi_c}$. The total area of the cell at time $\tau$ will be $|\Omega|(0) + \gamma_a A_g$. The latter corresponds to an increase of the side of an expanding square cell of magnitude $\sqrt{|\Omega|(0) + \gamma_a A_g} - \sqrt{|\Omega|(0)}$. Motivated by this we assume that the speed of the outer boundary should be proportional to the rate of increase of the above quantity. Namely, we have for $\mathsf{V}_e$ the speed of the moving boundary $\Gamma_e$

$$\mathsf{V_e} = \frac{\partial}{\partial \tau} \left( \sqrt{|\Omega|(0) + \gamma_a A_g(\tau)} \right). \tag{2.7}$$

[1] the mass/volume ratio of a porous material; that is, excluding the pore volume in contrast to bulk density which measures the mass/volume ratio that includes the cavities in a porous material, cf. [11].

https://doi.org/10.1017/S095679251800027X Published online by Cambridge University Press

At this point we should make the remark that considering one-dimensional cells and using a similar argument we would have that the speed of the outer cell boundary should be proportional to the rate of increase of the inner boundary and have $\mathsf{V_e} = -\gamma_a \mathsf{V}$ (cf. [5,22]) with $\Gamma_e$ initially being the points $-1$, 1.

Alternatively, for a cubic cell and now for $V_g = |\Omega_c|(0) - |\Omega_c|(\tau)$ the same argument results in taking $\mathsf{V_e} = \frac{\partial}{\partial \tau}\left(\sqrt[3]{|\Omega(0)| + \gamma_a V_g(\tau)}\right)$.

Moreover, we have to note that another, alternative and more simple modelling approach is to assume that at all times the outer boundary has the form of a square which is expanding. If its side is initially equal to $\sqrt{|\Omega|(0)} = 2$, then at time $\tau$, it should be, $2(1+\zeta(\tau))$ with $(2(1+\zeta))^2 = 4 + \gamma_a A_g(\tau)$. Thus, the position of the outer boundary can be determined at all times by the following algebraic equation

$$1 + \zeta(\tau) = \sqrt{1 + \frac{1}{4}\gamma_a A_g(\tau)}.$$

Although, to give more generality in the following analysis we will assume that the position of the outer boundary will be given from equation (2.7).

## 3 Homogenization

We next apply the method of homogenization for the model represented by the system of equations (2.3)–(2.7). The method of homogenization is a very powerful tool applied here to derive a macroscopic model. This form of homogenization [21], as well as similar homogenization methods as FE2 modelling [27] or distributed modelling [4] is part of a research area which has been immensely developed during the last decades. Moreover, this method allows us from the problem in the micro-scale to derive equations in the macroscopic scale. The latter equations will actually describe the corrosion process and more specifically the evolution of the mushy (mixed) region that is formed. By the term mushy (mixed) region we describe the region that corroded and uncorroded parts of the material coexist throughout the bulk of it, see [17,18] and [22–24].

We consider two spatial scales for the problem: a macroscopic length scale represented by the variable $y$ and a microscopic length scale represented by the variable $z$. Let $l$ be a typical macroscopic length scale, and $d$ the microscopic length scale. The scale $l$ can be taken to be a typical length of the observed corrosion in a time period of interest or a length associated with the thickness of material. In addition, the microscopic length scale $d$ can be taken to be of order of an average distance between two pores inside the material or the average diameter of a pore inside it.

Naturally, $d \ll l$ and their ratio is $\delta = \frac{d}{l} \ll 1$. More specifically, we have that for $x$ being the dimensional original distance, $x = ly$ and $x = dz$ with $\delta = \frac{d}{l} \ll 1$.

Moreover, the concentration $u$ is regarded as a function of both dimensionless distances, $y$ and $z$ as well as of time $\tau$ and $u = u(y, z, \tau)$. The multiple scales approach, see [14] gives, instead for the spatial derivative $\nabla_y u$ at the point $(y, z, t)$, the expression $\nabla_y u + \frac{1}{\delta}\nabla_z u$.

The boundary $\Gamma_c$ is assumed to be described by some function $\mathsf{s} = \mathsf{s}(y, \tau)$ ($\mathsf{s} = s/l$) for $s$ the dimensional boundary position. The position of the boundary $s$ can be rescaled with $d$ and we take $S = \frac{s}{d}$ ($= \frac{l}{d}\mathsf{s} = \frac{1}{\delta}\mathsf{s}$).

https://doi.org/10.1017/S095679251800027X Published online by Cambridge University Press

Rescaling also with $d$ the speed of the boundary $\mathsf{V}$, will give $\mathsf{V} = \delta\mathcal{V}$, where $\mathcal{V}$ is the new dimensionless variable for the speed (Dimensional boundary speed $= \mathsf{V}\,l/t_0 = \mathcal{V}\,d/t_0$, or $\mathsf{V} = \delta\mathcal{V}$). This implies that $\delta\mathcal{V} = R(u)$ on $\Gamma_c$.

If we denote with $\mathcal{S}$ the function representing the position of the boundary in the form $\mathcal{S}(y,z,\tau) = 0$, ( $\mathcal{S}(y,z,\tau) = z_2 - S(y,z_1,\tau) = 0$), we have that the rescaled speed of the boundary $\mathcal{V}$, [23] has the form

$$\delta\mathcal{V} = \frac{\partial\mathcal{S}}{\partial\tau}\frac{1}{|\nabla_z\mathcal{S} + \delta\nabla_y\mathcal{S}|}.$$

Application of the multiple scales method implies

$$\varepsilon u_\tau = \frac{1}{\delta^2}\nabla_z^2 u + \frac{2}{\delta}\nabla_y\nabla_z u + \nabla_y^2 u + f.$$

Regarding the Kinetic condition (2.4) we have at $\Gamma_c$,

$$\delta\mathcal{V} = \frac{\partial\mathcal{S}}{\partial\tau}\frac{1}{|\nabla_z\mathcal{S} + \delta\nabla_y\mathcal{S}|} = -\gamma_u\frac{1}{\delta^2}\,n\cdot\left[\nabla_z u + \delta\nabla_y u\right],$$

as well as, regarding equation (2.5),

$$\gamma_u\,n\cdot\left[\nabla_z u + \delta\nabla_y u\right] + \delta^2 R(u) = 0.$$

At the boundary $\Gamma_e$, similarly we have

$$n\cdot\left[\nabla_z u + \delta\nabla_y u\right]_{\Gamma_e^{1,2}} = n\cdot\left[\nabla_z u + \delta\nabla_y u\right]_{\Gamma_e^{3,4}},$$

$$u_{\Gamma_e^{1,2}} = u_{\Gamma_e^{3,4}}.$$

As for $\Gamma_c$ the position of the boundary $\Gamma_e$ can be expressed by a function $\mathcal{Z}(y,z,\tau) = 0$, with $\mathcal{Z}(y,z,\tau) = z_2 - Z(y,z_1,\tau) = 0$. The rescaled speed of the boundary $\Gamma_e$, $\mathcal{V}_e$, ($\mathsf{V}_e = \delta\mathcal{V}_e$) has the form

$$\delta\mathcal{V}_e = \frac{\partial\mathcal{Z}}{\partial\tau}\frac{1}{|\nabla_z\mathcal{Z} + \delta\nabla_y\mathcal{Z}|}.$$

In the following we proceed with a formal asymptotic expansion for $u$, $S$ and $Z$. Moreover, for the approximations that follow to be valid, we assume that the shape of the calcium carbonate core is not wildly fluctuating from cell to cell.

The equation for $u$, by assuming that $u \sim u_0 + \delta u_1 + \ldots$, $f = f_0 + \delta f_1 + \ldots$ takes the form

$$\begin{aligned}\epsilon u_{0\tau} + \ldots = {} & \frac{1}{\delta^2}\nabla_z^2 u_0 + \frac{2}{\delta}\nabla_z\nabla_y u_0 + \nabla_y^2 u_0 + f_0 \\ & + \frac{1}{\delta}\nabla_z^2 u_1 + 2\nabla_z\nabla_y u_1 + \nabla_z^2 u_2 + \ldots.\end{aligned}$$

At the points $(y,z,\tau)$ of the boundary $\Gamma_c$, we have for $\mathcal{S} = \mathcal{S}_0 + \delta\mathcal{S}_1 + \ldots$, and $|\nabla_z\mathcal{S} + \delta\nabla_y\mathcal{S}| = |\nabla_z\mathcal{S}_0 + \delta\nabla_y\mathcal{S}_0 + \delta\nabla_z\mathcal{S}_1 + \ldots|$, that

$$\frac{\partial\mathcal{S}_0}{\partial\tau}\frac{1}{|\nabla_z\mathcal{S}_0|} = -\gamma_u\,n\cdot\left[\frac{1}{\delta^2}\nabla_z u_0 + \frac{1}{\delta}\nabla_y u_0 + \frac{1}{\delta}\nabla_z u_1 + \nabla_y u_1 + \nabla_z u_2 + \ldots\right], \tag{3.2a}$$

https://doi.org/10.1017/S095679251800027X Published online by Cambridge University Press

$$R(u_0) + \cdots + \gamma_u n \cdot \left[\frac{1}{\delta^2}\nabla_z u_0 + \frac{1}{\delta}\nabla_y u_0 + \frac{1}{\delta}\nabla_z u_1 + \nabla_y u_1 + \nabla_z u_2\right] + \ldots = 0. \tag{3.2b}$$

Similarly, at the points $(y, z, \tau)$ of the boundary $\Gamma_e$ we have

$$n \cdot \left[\frac{1}{\delta^2}\nabla_z u_0 + \frac{1}{\delta}\nabla_y u_0 + \frac{1}{\delta}\nabla_z u_1 + \ldots\right]_{\Gamma_e^{1,2}} = n \cdot \left[\frac{1}{\delta^2}\nabla_z u_0 + \frac{1}{\delta}\nabla_y u_0 + \frac{1}{\delta}\nabla_z u_1 + \ldots\right]_{\Gamma_e^{3,4}} \tag{3.3a}$$

$$\left[u_0 + \delta u_1 + \delta^2 u_2 + \ldots\right]_{\Gamma_e^{1,2}} = \left[u_0 + \delta u_1 + \delta^2 u_2 + \ldots\right]_{\Gamma_e^{3,4}}. \tag{3.3b}$$

Additionally, regarding its motion we have that the corroded area is $A_g(\tau) = |\Omega_c|(0) - |\Omega_c|(\tau) = \int_0^1 (S(y, z_1, 0) - S(y, z_1, \tau))\, dz_1$ and

$$\frac{\partial \mathcal{Z}_0}{\partial \tau}\frac{1}{|\nabla_z \mathcal{Z}_0|} + \ldots = \frac{\partial}{\partial \tau}\left(\sqrt{1 + \frac{1}{4}\gamma_a \int_0^1 (S_0(y, z_1, 0) - S_0(y, z_1, \tau))\, dz_1}\right) + \ldots. \tag{3.4}$$

For order $O(\frac{1}{\delta^2})$ terms we have $\nabla_z^2 u_0 = 0$. By the conditions at the moving boundary $\Gamma_c$, that is, at $z = S$ we get $n \cdot \nabla_z u_0 = 0$. In addition, at the other boundary, the cell boundary $\Gamma_e$, we have periodic conditions $n \cdot \nabla_z u_0|_{\Gamma_e^{1,2}} = n \cdot \nabla_z u_0|_{\Gamma_e^{3,4}}$, $u_{0\Gamma_e^{1,2}} = u_{0\Gamma_e^{3,4}}$. By these equations and the maximum principle we deduce that $u_0 = u_0(y, \tau)$ in $\Omega_g$.

For order $O(\frac{1}{\delta})$ terms we have $2\nabla_z \nabla_y u_0 + \nabla_z^2 u_1 = 0 = \nabla_z^2 u_1 = 0$ in $\Omega_g$, given that $u_0 = u_0(y, \tau)$. Moreover, on $\Gamma_e$ the periodic conditions $n \cdot \left[\nabla_y u_0 + \nabla_z u_1\right]_{\Gamma_e^{1,2}} = n \cdot \left[\nabla_y u_0 + \nabla_z u_1\right]_{\Gamma_e^{3,4}}$, or $n \cdot [\nabla_z u_1]_{\Gamma_e^{1,2}} = n \cdot [\nabla_z u_1]_{\Gamma_e^{3,4}}$ and $u_1|_{\Gamma_e^{1,2}} = u_1|_{\Gamma_e^{3,4}}$ hold. Finally, on $\Gamma_c$ we obtain similarly $n \cdot \left[\nabla_y u_0 + \nabla_z u_1\right] = 0$ or $n \cdot [\nabla_z u_1] = -n \cdot \left[\nabla_y u_0\right]$. The latter condition gives a $z$ dependence on $u_1$, $u_1 = u_1(y, z, \tau)$.

In order to control the $z$-dependance of $u_1$, which comes from the fact that its gradient is proportional to $n \cdot \left[\nabla_y u_0\right]$ at the boundary, we define an auxiliary cell problem.

On writing $u_1 = w \cdot \nabla_y u_0$ for $w = w(z) = (w_1(z), w_2(z))$, we obtain the following cell problems

$$\nabla_z^2 w_i = 0, \quad \text{in} \quad \Omega_g, \tag{3.5a}$$

$$n \cdot \nabla_z w_i = -n_i, \quad \text{on} \quad \Gamma_c, \tag{3.5b}$$

$$[n \cdot \nabla_z w_i]_{\Gamma_e^{1,2}} = [n \cdot \nabla_z w_i]_{\Gamma_e^{3,4}}, \quad w_i|_{\Gamma_e^{1,2}} = w_i|_{\Gamma_e^{3,4}} \quad \text{on} \quad \Gamma_e, \tag{3.5c}$$

for $i = 1, 2$ and $n_i$ the directional cosines of the unit normal $n = (n_1, n_2)$. These cell functions actually are describing the effect of the shape, of the area in which diffusion takes place, to the overall diffusion coefficient.

Next for $O(1)$ terms, we have

$$\varepsilon u_{0\tau} = \nabla_y^2 u_0 + 2\nabla_z \nabla_y u_1 + \nabla_z^2 u_2 + f_0, \tag{3.6}$$

while at the boundary $\Gamma_c$,

$$\frac{\partial \mathcal{S}_0}{\partial \tau}\frac{1}{|\nabla_z \mathcal{S}_0|} = -\gamma_u n \cdot \left[\nabla_y u_1 + \nabla_z u_2\right] = R(u_0); \tag{3.7}$$

https://doi.org/10.1017/S095679251800027X Published online by Cambridge University Press

and similarly at the boundary $\Gamma_e$, we have

$$n \cdot \left[\nabla_y u_1 + \nabla_z u_2\right]_{\Gamma_e^{1,2}} = n \cdot \left[\nabla_y u_1 + \nabla_z u_2\right]_{\Gamma_e^{3,4}}, \quad u_2|_{\Gamma_e^{1,2}} = u_2|_{\Gamma_e^{3,4}}, \tag{3.8}$$

and

$$\frac{\partial \mathcal{Z}_0}{\partial \tau} \frac{1}{|\nabla_z \mathcal{Z}_0|} = \frac{\partial}{\partial \tau} \left( \sqrt{1 + \frac{1}{4}\gamma_a \int_0^1 (S_0(y, z_1, 0) - S_0(y, z_1, \tau))\, dz_1} \right). \tag{3.9}$$

We next proceed by averaging the field equation (3.6) over the whole domain occupied by the pore-gypsum area, say $\Omega_g$. That is, we integrate both sides with respect to $z$ over $\Omega_g$ to eliminate the $z$-dependence from the equations.

$$\int_{\Omega_g} \left[\varepsilon u_{0\tau} - \nabla_y^2 u_0 - 2\nabla_z \nabla_y u_1 - f_0\right] dz = \int_{\Omega_g} \nabla_z^2 u_2 dz = \int_{\Gamma_c \cup \Gamma_e} n \cdot \nabla_z u_2 ds. \tag{3.10}$$

Note here that

$$\int_{\Omega_g} \left[2\nabla_z \cdot \nabla_y u_1\right] dz = \int_{\Omega_g} 2\nabla_z \cdot \nabla_y \left(w \cdot \nabla_y u_0\right) dz = \left(2 \int_{\Omega_g} \nabla_z \cdot w\, dz\right) \nabla_y^2 u_0,$$

and additionally, in view of the relation $\int_{\Gamma_e} n \cdot \nabla_z \cdot u_2 dz = 0$ and of the second part of equation (3.7), we have

$$\begin{aligned}
\int_{\Gamma_c \cup \Gamma_e} n \cdot \nabla_z u_2 ds &= \int_{\Gamma_c} n \cdot \nabla_z u_2 ds = \int_{\Gamma_c} \left[-n \cdot \nabla_y u_1 - \frac{1}{\gamma_u} R(u_0)\right] ds \\
&= \int_{\Gamma_c} \left[-n \cdot \nabla_y \left(w \cdot \nabla_y u_0\right)\right] ds - \frac{1}{\gamma_u} \int_{\Gamma_c} R(u_0) ds \\
&= -\nabla_y^2 u_0 \int_{\Gamma_c} [n \cdot w]\, ds - \frac{1}{\gamma_u} R(u_0) \int_{\Gamma_c} ds \\
&= -\nabla_y^2 u_0 \left(\int_{\Omega_g} \nabla_z \cdot w\, dz\right) - \frac{1}{\gamma_u} R(u_0) |\Gamma_c|,
\end{aligned}$$

for $|\Gamma_c| = \int_{\Gamma_c} ds$.

Combining the above relations with equation (3.10) we obtain

$$\varepsilon u_{0\tau} \int_{\Omega_g} dz = \left[\int_{\Omega_g} dz + \int_{\Omega_g} \nabla_z w dz\right] \nabla_y^2 u_0 - \frac{1}{\gamma_u} R(u_0) |\Gamma_c| + f_0 \int_{\Omega_g} dz, \tag{3.11}$$

or

$$\varepsilon u_{0\tau} = \left[1 + \frac{1}{|\Omega_g|} \int_{\Omega_g} \nabla_z \cdot w dz\right] \nabla_y^2 u_0 - \frac{1}{\gamma_u} \frac{|\Gamma_c|}{|\Omega_g|} R(u_0) + f_0, \tag{3.12}$$

for $|\Omega_g| = \int_{\Omega_g} dz$.

On summarizing the final set of equations that are derived by this process, modelling

https://doi.org/10.1017/S095679251800027X Published online by Cambridge University Press

corrosion in a macroscopic scale is

$$\varepsilon\frac{\partial u_0}{\partial\tau}(y,\tau)=D(y,\tau)\nabla_y^2u_0(y,\tau)-\tfrac{1}{\gamma_u}\frac{L(y,\tau)}{A(y,\tau)}R(u_0)+f_0\quad\text{in}\quad\Omega_g,$$
$$\frac{\partial\mathcal{S}_0}{\partial\tau}\frac{1}{|\nabla_z\mathcal{S}_0|}=R(u_0)\quad\text{on}\quad\Gamma_c,$$
$$\frac{\partial\mathcal{Z}_0}{\partial\tau}\frac{1}{|\nabla_z\mathcal{Z}_0|}=\frac{\partial}{\partial\tau}\left(\sqrt{1+\tfrac{1}{4}\gamma_a\int_0^1\left(S_0(y,z_1,0)-S_0(y,z_1,\tau)\right)dz_1}\right)\quad\text{on}\quad\Gamma_e,$$

for $D(y,\tau)=\left[1+\frac{1}{|\Omega_g|}\int_{\Omega_g}\nabla_z\cdot w\,dz\right]$, $A(y,\tau)=\frac{1}{\phi_g}|\Omega_g|$, $L(y,\tau)=\frac{1}{\phi_g}|\Gamma_c|$.

The area $A(y,\tau)$ is determined as the area between the boundaries $\Gamma_c$ and $\Gamma_e$.

Moreover, by the fact that to first order terms we have $\mathcal{S}=z_2-S(y,z_1,\tau)\simeq\mathcal{S}_0$, $\mathcal{Z}=z_2-Z(y,z_1,\tau)\simeq\mathcal{Z}_0$, we get

$$L(y,\tau)=\int_{\Gamma_c}dz=4\int_0^1\sqrt{1+\left(\frac{\partial S}{\partial z_1}\right)}dz_1,$$
$$A(y,\tau)=4\left[\int_0^1Z(y,z_1,\tau)dz_1-\int_0^1S(y,z_1,\tau)dz_1\right].$$

The term $\int_0^1\sqrt{1+\left(\frac{\partial S}{\partial z_1}\right)}dz_1$ in the above equation gives the length of the inner boundary in the first quadrant and, therefore, to get the full length of the boundary $L(y,\tau)$ we multiply by four. The same applies for $A(y,\tau)$.

### 3.1 Overall change in porosity

An additional aspect we have to account for is the change of the porosity $\phi=\phi(y,\tau)$ during the process and due to the transformation of calcite to gypsum. We must have a variation of the porosity in one cell from $\phi_c$ initially (porosity of the uncorroded material) to $\phi_g$ (gypsum porosity) at the end of the process. Also the maximum expansion of the cell area will be achieved when all of the calcium carbonate has been transformed into gypsum. Furthermore, the gypsum created is distributed in such a way so that new void space (new islets of void space) is created, expanding the total cell area. The additional final area should be $\gamma_a\times Initial\ core\ area=\gamma_a(4-A(y,0))$ and the total cell area becomes $4+\gamma_a(4-A(y,0))$, for $\Omega(0)=4$ and $4-A(y,0)$ the initial calcite core area.

The total area of the cell at time $\tau$, in terms of $A(y,\tau)$, is

$$\begin{aligned}|\Omega|(\tau)&=|\Omega|(0)+\gamma_a\left(|\Omega_c|(0)-|\Omega_c|(\tau)\right)=|\Omega|(0)+\gamma_a\left(\left(|\Omega|(0)-A(y,0)\right)-\left(|\Omega|(\tau)-A(y,\tau)\right)\right)\\&=-\gamma_a|\Omega|(\tau)+(1+\gamma_a)\Omega|(0)+\gamma_a\left(A(y,\tau)-A(y,0)\right)\\&=|\Omega|(0)+\left(\gamma_a/(1+\gamma_a)\right)\left(A(y,\tau)-A(y,0)\right).\end{aligned}$$

Therefore, we have

$$\begin{aligned}\phi(y,\tau)&=\frac{\text{Initial Void + Additional void created at time }\tau}{\text{Initial cell volume +Additional area due to expansion at time }\tau}\\&=\frac{4\phi_c+\gamma_v\left(A(y,\tau)-A(y,0)\right)}{4+\left(\gamma_a/(1+\gamma_a)\right)\left(A(y,\tau)-A(y,0)\right)},\end{aligned}$$

https://doi.org/10.1017/S095679251800027X Published online by Cambridge University Press

for $\phi_c = A(y,0)/4$, $\gamma_v$ a factor to be determined appropriately and for the additional void created written in terms of $(A(y,\tau) - A(y,0))$. More specifically we have at the end of the process $\phi_g = \frac{4\phi_c+\gamma_v(4(1+\gamma_a(1-\phi_c))-A(y,0)))}{4+(\gamma_a/(1+\gamma_a))(4(1+\gamma_a(1-\phi_c))-A(y,0))}$, which gives $\gamma_v = \frac{\gamma_a}{1+\gamma_a}\phi_g + \frac{1}{1+\gamma_a}\frac{\phi_g-\phi_c}{1-\phi_c}$.

### 3.2 Boundary conditions

In the following and in order to complete the model equations, we need to impose appropriate boundary conditions. Also we have to take into account the fact that during the process, in the macro-scale, the porosity changes at each point $(y,\tau)$. The derived equations account for the actual concentration of $u$, while the effective concentrations of it, $\bar{u}$, is given by $\bar{u} = \phi u$. The total domain of the material under study is $\Omega_M$ and we may take the boundary of $\Omega_M$ or part of it, exposed to the ambient concentration of the pollutant. In this case we can impose standard Dirichlet conditions at the boundary $\partial\Omega_M$ of the form $\bar{u} = \phi u = c(t)$. Where $c(t)$ the outer concentration of the pollutant possible varying with time during the period of the study. For simplicity we can use an average value in place of $c(t)$ and get $\bar{u} = \phi u = 1$ after an appropriate scaling of $u$.

Furthermore, in the very common case that we have planar propagation of the corrosion the domain $\Omega_M$ can be taken as one dimensional and have $\Omega_M = [0,1]$, at $\tau = 0$, after appropriate scaling.

In addition, we have expansion of the domain due to its change in the porosity and in such a case we have to take $\Omega_M(\tau) = [-\alpha(\tau), 1]$, for $\alpha(\tau)$ expressing the shift of the macroscopic boundary to the left due to swelling. Then, we should have $\phi(-\alpha(\tau),\tau)\,u(-\alpha(\tau),\tau) = 1$. At the other end $y = 1$, we can impose Neumann conditions $\bar{u}_y = (\phi u)_y = 0$ due to an assumption of symmetry (having an one-dimensional bar corroded from both ends) or due the fact that we have some kind of insulation at this end, that is a material that cannot be corroded for $y \geqslant 1$.

### 3.3 Expansion of the macroscopic boundary

The increase of the porosity of each cell causes the expansion of the volume of that cell and therefore at each point $(y,\tau)$ the change in porosity $d\phi(y,\tau)$ will cause a corresponding increase in swelling, and specifically in the position of the outer boundary $\alpha(\tau)$. By summing up these contributions, we can obtain an estimation of $\alpha(\tau)$. Consequently, following this point of view, $\alpha(\tau)$ is expected to be proportional to the overall change of the porosity of the material, namely we have

$$\alpha(\tau) = \frac{\gamma_a}{1/(1-\phi_c)+\gamma_a}\int_{-\alpha(\tau)}^{1}\frac{\phi(y,\tau)-\phi_c}{\phi_g-\phi_c}dy.$$

According to this relation, for $\phi(y,0) = \phi_c$ we have $\alpha(0) = 0$ and when the transformation to gypsum is complete, after some time $\tau_c$, we expect swelling of size $\gamma_a(1-\phi_c)$. Indeed for $\phi(y,\tau) = \phi_g$, for every $y \in \Omega_M$ and for time $\tau \geqslant \tau_c$, we have $\frac{\gamma_a}{1/(1-\phi_c)+\gamma_a}(1+\alpha(\tau)) = \alpha(\tau)$ or that $\alpha(\tau) = \gamma_a(1-\phi_c)$.

Summarizing, the equations derived, for the case that we consider one dimension in the macro-scale, and by dropping the subscripts in the notation for $u$, $\mathcal{S}$ and $\mathcal{Z}$ since $u \simeq u_0$,

https://doi.org/10.1017/S095679251800027X Published online by Cambridge University Press

$\mathcal{S}\simeq\mathcal{S}_0$, $\mathcal{Z}\simeq\mathcal{Z}_0$, we have that the upscaled (limit) model takes the following form:

$$\epsilon u_\tau - D(y,\tau)u_{yy} - f_0(y,\tau) = -\frac{1}{\gamma_u}R(u)\frac{L(y,\tau)}{A(y,\tau)}, \quad -\alpha(\tau) < y < 1, \quad \tau \geqslant 0, \tag{3.13a}$$

$$u(-\alpha,\tau) = \frac{1}{\phi(-\alpha,\tau)}, \quad u_y(1,\tau) + \frac{\phi_y(1,\tau)}{\phi(1,\tau)}u(1,\tau) = 0, \tag{3.13b}$$

$$u(y,0) = u_a(y), \tag{3.13c}$$

$$-\frac{\partial S}{\partial \tau}\frac{1}{\sqrt{1+\left(\frac{\partial S}{\partial z_1}\right)^2}} = R(u), \quad 0 < z_1 < 1, \quad \tau \geqslant 0, \tag{3.13d}$$

$$S(y,z_1,0) = S_a(z_1), \quad \frac{\partial S}{\partial z_1}(y,0,\tau) = 0, \tag{3.13e}$$

$$\frac{\partial Z}{\partial \tau}\frac{1}{\sqrt{1+\left(\frac{\partial Z}{\partial z_1}\right)^2}} = \frac{\partial}{\partial \tau}\sqrt{1+\frac{1}{4}\gamma_a\int_0^1 (S(y,z_1,0)-S(y,z_1,\tau))\,dz_1},$$

$$1 < z_1 < 1+\gamma_a, \quad \tau \geqslant 0, \tag{3.13f}$$

$$Z(y,z_1,0) = Z_a(z_1), \quad \frac{\partial Z}{\partial z_1}(y,0,\tau) = 0, \tag{3.13g}$$

$$L(y,\tau) = 4\int_{S(y,z_1,\tau)} dz_{\Gamma_s}, \quad A(y,\tau) = 4\left[\int_0^1 Z(y,z_1,\tau)dz_1 - \int_0^1 S(y,z_1,\tau)dz_1\right], \tag{3.13h}$$

$$\phi(y,\tau) = \frac{4\phi_c + \gamma_v\,(A(y,\tau)-A(y,0))}{4+(\gamma_a/(1+\gamma_a))\,(A(y,\tau)-A(y,0))}, \tag{3.13i}$$

$$\alpha(\tau) = \frac{\gamma_a}{1/(1-\phi_c)+\gamma_a}\int_{-\alpha(\tau)}^1 \frac{\phi(y,\tau)-\phi_c}{\phi_g-\phi_c}dy. \tag{3.13j}$$

$$D(y,\tau) = \left[1+\frac{1}{\phi_g A(y,\tau)}\int_{\Omega_g}\nabla_z w(z)dz\right] \tag{3.13k}$$

$$\nabla_z^2 w_i = 0, \quad \text{in} \quad \Omega_g(y,\tau), \quad w=(w_1,w_2),\ i=1,2, \tag{3.13l}$$

$$n\cdot\nabla_z w_i = 0, \quad \text{on} \quad \Gamma_e, \quad n\cdot\nabla_z w_i = -n_i, \quad \text{on} \quad \Gamma_c(y,\tau). \tag{3.13m}$$

Here, $u_a$ is the initial condition for $u$ and a natural choice to make is to take $u_a = 0$. Also, $S_a$ is the initial position of the moving boundary $\Gamma_c$, applied to all the cells inside the material, assumed to be independent of $y$, while for $\tau > 0$ its position is given by the points $(z_1, z_2)$ for which we have $z_2 = S(y,z_1,\tau)$. Similarly, $Z_a$ is the initial position of $\Gamma_e$. The range of $z_1$ in (3.13*c*), (3.13*f*) is determined by the fact that $S$ is shrinking and $Z$ expanding.

## 4 Transformation to a fixed domain and variations of the model

### 4.1 Change of time variable in the Eikonal equation

In order to simplify the analysis, as well as the numerical treatment of the problem, we proceed with a change in time variable in the equations for the moving boundaries (3.13*d*), (3.13*f*) [23, 24].

https://doi.org/10.1017/S095679251800027X Published online by Cambridge University Press

More precisely in (3.13*c*) we set $\frac{\partial S}{\partial \tau} = \frac{\partial S}{\partial \sigma}\frac{\partial \sigma}{\partial \tau}$, for $\sigma$ a new time variable. Thus, we obtain

$$-\frac{\partial S}{\partial \sigma}\frac{\partial \sigma}{\partial \tau} = R(u)\sqrt{1+\left(\frac{\partial S}{\partial z_1}\right)^2},\ S(y,z_1,0) = S_a(z_1),\ \frac{\partial S}{\partial z_1}(y,0,\tau) = 0.$$

Then, we set $\frac{\partial \sigma}{\partial \tau} = R[u(y,\tau)] = R(y,\tau)$ or

$$\sigma = \sigma(y,\tau) = \int_0^\tau R(y,\tau')d\tau', \tag{4.1}$$

and we obtain a form of the Eikonal equation $\left(\left(\frac{\partial S}{\partial \sigma}\right)^2 - \left(\frac{\partial S}{\partial z_1}\right)^2 = 1\right)$ for $S = S(z_1,\sigma)$,

$$-\frac{\partial S}{\partial \sigma} = \sqrt{1+\left(\frac{\partial S}{\partial z_1}\right)^2}, \quad 0 < z_1 < 1, \quad \sigma \geqslant 0, \tag{4.2a}$$

$$S(z_1,0) = S_a(z_1), \quad S_{z_1}(0,\sigma) = 0. \tag{4.2b}$$

Similarly, for the boundary $\Gamma_e$, we obtain for $Z = Z(z_1,\sigma)$

$$\frac{\partial Z}{\partial \sigma} = \sqrt{1+\left(\frac{\partial Z}{\partial z_1}\right)^2}\frac{\partial}{\partial \sigma}G(\sigma), \quad 0 < z_1, \quad \sigma \geqslant 0, \tag{4.3a}$$

$$\text{for} \quad G(\sigma) = \sqrt{1+\frac{1}{4}\gamma_a\int_0^1 (S(z_1,0) - S(z_1,\sigma))\,dz_1},$$

$$Z(z_1,0) = Z_a(z_1), \quad Z_{z_1}(0,\sigma) = 0. \tag{4.3b}$$

### 4.2 Sandpile Solution for $\Gamma_e$

Given the assumption that the cells inside the material have the specified form of a square, the Eikonal equation for $\Gamma_e$ attains analytical solutions (sandpile solutions [15,23]). For a square cell, say of side 2, we have $Z_a(z_1) = 1$, for $0 < z_1 < 1$. Assuming that this has the form $Z = 1 + h(\sigma)$ we obtain that $\frac{dh}{d\sigma} = \frac{\partial}{\partial \sigma}G(\sigma)$ with $h(0) = 0$ and $G(0) = 1$. Therefore, $h(\sigma) = G(\sigma) - 1$, $Z(z_1,\sigma) = G(\sigma)$, or

$$Z(y,z_1,\tau) = G\left(\int_0^\tau R(y,\tau')d\tau'\right). \tag{4.4}$$

Note also that due to the symmetry of the square element, we need at $Z = z_1$, the free boundaries to intersect. Thus, we have $Z = G(\sigma)$ for $0 \leqslant z_1 \leqslant G(\sigma)$. The moving boundary stops to expand for $\sigma = \sigma_f$ the time needed for $S$ to vanish and have $G(\sigma_f) = \left(\sqrt{1+\frac{1}{4}\gamma_a\int_0^1 (S(z_1,0))\,dz_1}\right)$. Then, the whole of the square element has been transformed into gypsum.

This form of $Z$ imply that in the system (3.13) equations (3.13*f*), (3.13*g*) can be replaced

https://doi.org/10.1017/S095679251800027X Published online by Cambridge University Press

by (4.4) and in addition the second relation in (3.13*h*) can also be replaced by

$$A(y,\tau) = 4\left[G^2\left(\int_0^\tau R(y,\tau')d\tau'\right) - \int_0^1 S(y,z_1,\tau)dz_1\right]. \tag{4.5}$$

### 4.3 Sandpile solutions for the inner boundary

Furthermore, given a specific initial interface $S_a$, we can obtain analytical solutions of equation (4.2) [23]. In such a case in the end we obtain a non-local in time form of equation (3.13*a*). For the cases of our interest we present them briefly.

*Square Segment*

Assuming that the calcite segment is a square of side $2L_0$ cantered in the cell of initial side 2, such that $\frac{4-(2L_0)^2}{4} = \phi_c$ or $L_0 = \sqrt{1-\phi_c}$, we set $S_a(z_1) = S(z_1,0) = L_0$ for $0 < z_1 < 1$. Then, as for the outer boundary $\Gamma_e$, the solution of equation (4.2) is $S(z_1,\sigma) = L_0 - \sigma$ for $0 \leqslant z_1 \leqslant L_0 - \sigma$, or $S(y,z_1,\tau) = L_0 - \int_0^\tau R(y,\tau')\,d\tau'$.

Thus, for $L$ and $A$, the first of equation (3.13*h*), and (4.5) become

$$L(y,\tau) = 8\left[L_0 - \int_0^\tau R(y,\tau')d\tau'\right],$$
$$A(y,\tau) = 4\left[G^2\left(\int_0^\tau R(y,\tau')d\tau'\right) - \left(L_0 - \int_0^\tau R(y,\tau')d\tau'\right)^2\right].$$

Substitution of these expressions in (4.6) and applying the transformation from $y$ to $r$, results in a nonlocal in time problem.

*Cyclical Segment*

The same can be done for the case that the initial calcite segment has the form of a cycle. In such a case $S_a = S(z_1,0) = \sqrt{R_0^2 - z_1^2}$, for $0 < z_1 < 1$. Then, the solution of (4.2) is

$$S(y,z_1,\tau) = \left[\left(R_0 - \int_0^\tau R(y,\tau')\,d\tau'\right)^2 - z_1^2\right]^{\frac{1}{2}},$$

for $0 < z_1 < R_0 - \sigma = R_0 - \int_0^\tau R(y,\tau')\,d\tau'$. Therefore, we have

$$L(y,\tau) = 2\pi\left[R_0 - \int_0^\tau R(y,\tau')\,d\tau'\right]$$
$$A(y,\tau) = 4\left[G^2\left(\int_0^\tau R(y,\tau')d\tau'\right) - \frac{\pi}{4}\left(R_0 - \int_0^\tau R(y,\tau')\,d\tau'\right)^2\right].$$

https://doi.org/10.1017/S095679251800027X Published online by Cambridge University Press

### 4.4 Transformation to a fixed domain

Another aspect that we have to address in system (3.13) is that in the field equation (3.13*a*) the domain $\Omega_M = [-\alpha(\tau), 1]$ is varying with time. One way to treat this is to transform the varying domain to a fixed one. This will allow us also to tackle the problem numerically. For this purpose we use the new spatial variable, $r$, by setting

$$r = \frac{y + \alpha(\tau)}{1 + \alpha(\tau)},$$

so that $r = 0$ for $y = -\alpha(\tau)$ and $r = 1$ for $y = 1$. In addition, we have $\frac{\partial}{\partial y} = \frac{1}{1+\alpha(\tau)}\frac{\partial}{\partial r}$, $\frac{\partial^2}{\partial y^2} = \frac{1}{(1+\alpha(\tau))^2}\frac{\partial^2}{\partial r^2}$, $u_\tau(y,\tau) = u_\tau(r,\tau) + \dot{\alpha}(\tau)\frac{1-r}{1+\alpha(\tau)}u_r(r,\tau)$ and equation (3.13*a*) takes the form

$$\epsilon u_\tau + \dot{\alpha}(\tau)\frac{1-r}{1+\alpha(\tau)}u_r - \frac{D(r,\tau)}{(1+\alpha(\tau))^2}u_{rr} - f_0(r,\tau) = -\frac{1}{\gamma_u}R(u)\frac{L(r,\tau)}{A(r,\tau)}, \tag{4.6}$$

for $0 < r < 1, \quad \tau \geqslant 0$.

Moreover, with this spatial transform we get an easier to handle, form of equation (3.13*j*), that is

$$\alpha(\tau) = \frac{\gamma_a}{1/(1-\phi_c) + \gamma_a}\int_0^1 \frac{\phi(r,\tau) - \phi_c}{\phi_g - \phi_c}(1 + \alpha(\tau))\,dr$$

or

$$\alpha(\tau) = \frac{\Phi(\tau)}{\frac{1/(1-\phi_c)+\gamma_a}{\gamma_a} - \Phi(\tau)}, \quad \text{for} \quad \Phi(\tau) = \frac{\int_0^1 \phi(r,\tau)dr - \phi_c}{\phi_g - \phi_c}. \tag{4.7}$$

Finally, the first of the boundary conditions, (3.13*b*) holds for $r = 0$, while the second of them remains invariant, namely

$$u(0,\tau) = \frac{1}{\phi(0,\tau)}, \quad u_r(1,\tau) + \frac{\phi_r(1,\tau)}{\phi(1,\tau)}u(1,\tau) = 0. \tag{4.8}$$

These equations (4.6), (4.8), (in place of (3.13*a*), (3.13*b*)) and (3.13*c*) for $u$, with the improved form of the equations for the moving boundaries, (4.1), (4.2), (in place of (3.13*d*), (3.13*e*) ) and (4.4) (in place of (3.13*f*), (3.13*g*)), the first of (3.13*h*) and (4.5) for the gypsum area, equation (3.13*i*) for the porosity $\phi$, equation (4.7) for the macroscopic moving boundary (in place of (3.13*j*)) together with (3.13*k*), (3.13*l*) and (3.13*m*), form the transformed to a fixed domain, model.

## 5 Numerical solution

We treat numerically the problem by following similar methodology as in [23, 24]. We apply a process in three stages.

Initially, we need to solve the Eikonal equation (4.2) for the cases that we cannot obtain an analytical solution. This can be done by using a level set method for a time range $0 \leqslant \sigma \leqslant \sigma_f$.

https://doi.org/10.1017/S095679251800027X Published online by Cambridge University Press

At a second stage having obtain the solution for the inner boundary we need to solve the auxiliary cell problems, that is equations (3.13*l*), (3.13*m*), for a sequence of domains $\Omega_g(y,\sigma_i)$, where $\sigma_i$ correspond to the points of a partition of $[0,\sigma_f]$. This is done with a finite element method.

Finally, we use these solutions, $S$ and $w$, to evaluate the source terms in the macroscopic equation for $u$ and to solve the resulting problem via an implicit in time finite element scheme.

*Level set method for the Eikonal equation.* We take a partition of $[-1,1]\times[-1,1]$ of $(M_\sigma+1)^2$ points $z_{1,2_j}=j\delta z_{1,2}$, with $\delta z_1=\delta z_2$, being the spatial steps and for $j=0,1,2,\ldots,M_\sigma$. Let $T_\sigma$ being the final time of the simulation. Similarly, in the interval $[0,T_\sigma]$, we take a partition with $N_\sigma$ time steps of size $\delta\sigma$ for $N_\sigma=\left[\frac{T_\sigma}{\delta_\sigma}\right]$ and $\sigma_\ell=\ell\delta\sigma$, $\ell=1,2,\ldots,N_\sigma$.

We denote with $S^\ell_{i,j}$ the approximation of $S(z_{1i},z_{2j},\sigma_\ell)$, $i,j=0,1,2,\ldots,M_\sigma$, $\ell=1\ldots N_\sigma$. According to a level set method, see [19, 25], and recalling that $\mathcal{S}=z_2-S(y,z_1,\tau)$, with $\frac{\partial\mathcal{S}}{\partial\sigma}=|\nabla_z\mathcal{S}|$ we have

$$
\begin{aligned}
&D^+_{z_1}\mathcal{S}^\ell_{i,j}=\left(\mathcal{S}^\ell_{i+1,j}-\mathcal{S}^\ell_{i,j}\right)/\delta z_1,\quad D^-_{z_1}\mathcal{S}^\ell_{i,j}=\left(\mathcal{S}^\ell_{i,j}-\mathcal{S}^\ell_{i-1,j}\right)/\delta z_1,\\
&D^+_{z_2}\mathcal{S}^\ell_{i,j}=\left(\mathcal{S}^\ell_{i,j+1}-\mathcal{S}^\ell_{i,j}\right)/\delta z_2,\quad D^-_{z_2}\mathcal{S}^\ell_{i,j}=\left(\mathcal{S}^\ell_{i,j}-\mathcal{S}^\ell_{i,j-1}\right)/\delta z_1,\\
&H=\sqrt{\min(0,D^-_{z_1}\mathcal{S}^\ell_{i,j})^2+\max(0,D^+_{z_1}\mathcal{S}^\ell_{i,j})^2+\min(0,D^-_{z_2}\mathcal{S}^\ell_{i,j})^2+\max(0,D^+_{z_2}\mathcal{S}^\ell_{i,j})^2},\\
&\mathcal{S}^{\ell+1}_j=\mathcal{S}^\ell_j-\delta\sigma\,H\quad i,j=1\ldots,M_\sigma-1,\quad \ell=1\ldots N_\sigma.
\end{aligned}
\tag{5.1}
$$

For the stability of the above scheme the condition $(\delta\sigma/\delta z_1+\delta\sigma/\delta z_2)\leqslant 1/2$ should be satisfied. In Figure 3 we plot the numerical solution of the Eikonal equation in the case that we have as an initial curve a Lame curve of the form $z_1^n+z_2^n=C$ [16]. The curve shrinks towards the centre of the square.

This solution must be expressed in terms of the time variable $\tau$. In order to do so we take a grid for the macroscopic domain $[0,T]\times[0,1]$. We have for $0\leqslant\tau\leqslant T$, $\tau_n=n\delta\tau$, $\delta\tau=\left[\frac{T}{N}\right]$ and for $N$ the time steps. Also, for $0\leqslant r\leqslant 1$ we take $M+1$ points $r_j=j\delta r$, $j=0,1,\ldots,M$ for $\delta r$ the spatial step.

Given the approximation of $\mathcal{S}(z_1,z_2,\sigma)=z_2-S(z_1,\sigma)$ at the point $(z_{1j},\sigma_\ell)$, $S^\ell_j$, in terms of $\sigma$ (restricted in the quarter domain $[0,1]\times[0,1]$ due to symmetry), with $S^\ell:=\left(S^\ell_1,S^\ell_2,\ldots,S^\ell_{M_\sigma}\right)$, we are able to calculate the quantities $L$ and $A$ in the source term in the equation for $u$ at each time step. We determine (interpolate) for each $(r_j,\tau_i)$ the corresponding $\sigma_\ell$ so that $A(r_j,\tau_i)=I_A(\sigma_\ell):=\int_0^1 S(z_1,\sigma_\ell)dz_1$ and $L(r_j,\tau_i)=I_L(\sigma_\ell):=\int_{S^\ell}S(z_1,\sigma_\ell)dz_1$. The index $\ell$ of $\sigma_\ell$ that corresponds to the point $(r_j,\tau_i)$ is the one that minimizes the quantity $(\sigma_\ell-I^j_{\tau_i})$, for $I^j_{\tau_i}:=\int_0^{\tau_i}R(r_j,\tau')d\tau'$.

*Finite element method for the cell problems.* The next stage is to solve numerically the cell problems for $w$, (3.13*k*) and (3.13*l*). We have obtained the solution of the Eikonal equation. Namely we know the position of the inner boundary $S$ together of course with the position of the outer boundary $Z$. This allow us to identify at each time step $\sigma_\ell$, in a partition of the interval $[0,T_\sigma]$, the domain $\Omega_g=\Omega_g(\sigma)$. Then, for this domain we use a finite element scheme to solve these cell problems. The finite element numerics package in MATLAB 'Distmesh' [26] is used to triangulate $\Omega_g(\sigma)$. Then, a solver that has been

https://doi.org/10.1017/S095679251800027X Published online by Cambridge University Press

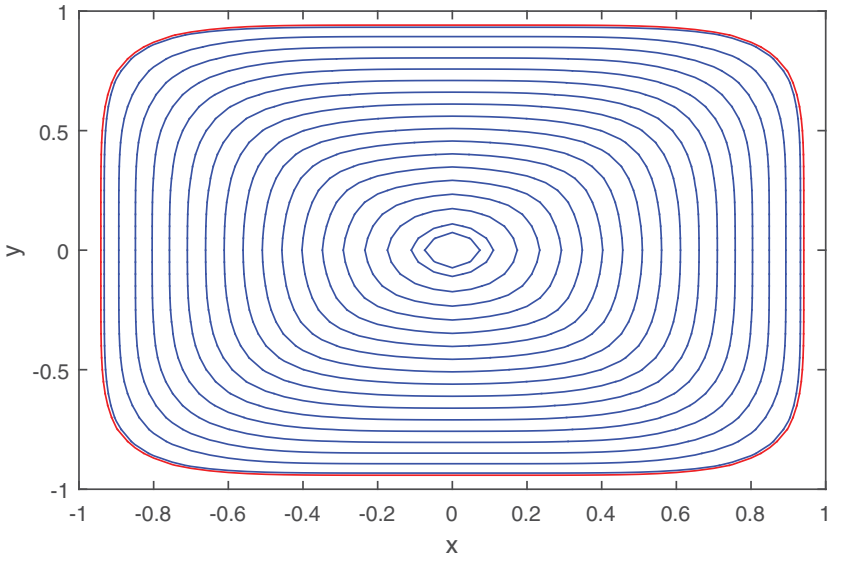


FIGURE 3. Numerical solution for the Eikonal equation. The initial curve (red line) is $z_1^n + z_2^n = C$ for $n = 6$ and $C = 0.7$. The solution is plotted for various times. As time increases the curve shrinks towards the centre of the cell. Here, $\delta z_{1,2} = 0.05$, $\delta\sigma = 0.0075$.

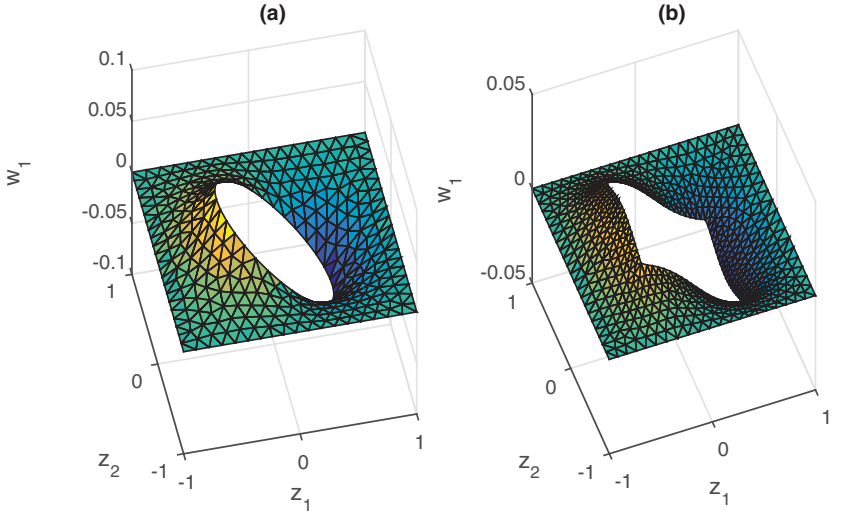


FIGURE 4. Numerical solution via a finite element method for a cell problem. In (a) the problem (3.13*k*) and (3.13*l*), for $w_1$ is solved in the case that the inner boundary is a circle of radius $R = 0.5$. In (b) the same problem is solved in the case that the inner interface is a square of side $2L_0 = 0.5$.

implemented for this specific problem (equations (3.13*k*), (3.13*l*)) is applied. An example of such a numerical solution for this problem is presented in Figure 4.

As a next step we can evaluate the variable diffusion coefficient given by equation (3.13*k*). In the graphs of Figure 5 we can see the variation of $D(y, \tau)$ against the gypsum-void area $|\Omega_g|$. In the case that the initial calcite core (inner boundary) is taken to be a

https://doi.org/10.1017/S095679251800027X Published online by Cambridge University Press

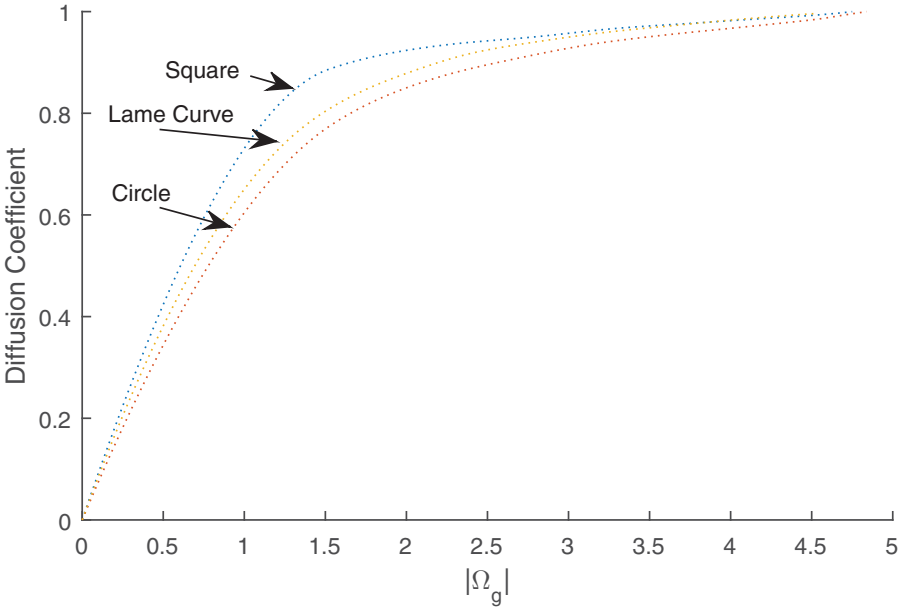


FIGURE 5. Numerical estimation of the diffusion coefficient $D$ given by equation (3.13$k$) against $|\Omega_g|$. The diffusion coefficient is plotted for the cases that the initial calcite core is a square, a circle and a Lame curve.

circle or a square, the analytical sandpile solutions is used. For the case that the initial calcite core is taken with a form that we cannot have analytical solution of the Eikonal equation, for example, a Lame curve with equation $z_1^n + z_2^n = C$ as in Figure 3, it uses the numerical solution obtained with a level set method. In this way the positions of the inner boundary is determined and consequently $|\Omega_g|$. In the latter case and for a Lame curve the initial area is given by $\sqrt{\frac{\Gamma(1+2/n)}{4\Gamma(1+1/n)}}$. The expansion of the outer cell boundary given by the relevant sandpile solution is also considered in all of the above cases.

*Finite element scheme for the field equations.* In the third stage, we use a finite element scheme to solve the field equation (4.6) together with its boundary and initial conditions. Let $\psi_j = \psi_j(r)$, $j = 0, \ldots, M$ denote the standard linear B – splines on the interval [0, 1], defined with respect to the partition considered. We then set $u(r,\tau) = \sum_{j=0}^{M} a_{u_j}(\tau)\psi_j(r)$, $\tau \geqslant 0$, $0 \leqslant r \leqslant 1$. We apply the standard Galerkin method and obtain a system of equations for the $a$'s. We also denote by $F$, the source term in the equation for $u$. Specifically, $F(u) := -1/\gamma_u \times R(u)\, L/A + f_0$.

$$\epsilon \sum_{j=0}^{M} \dot{a}_{u_j} \int_0^1 \psi_j\, \psi_i\, dr = -\frac{1}{(1+\alpha)^2} \sum_{j=0}^{M} a_{u_j} \int_0^1 D(r,\tau)\psi_j'\, \psi_i'\, dr - \frac{\dot{\alpha}}{1+\alpha} \sum_{j=0}^{M} a_{u_j} \int_0^1 (1-r)\psi_j'\, \psi_i\, dr + \int_0^1 F\left(\sum_{j=0}^{M} a_{u_j}\psi_j\right) \psi_i\, dr, \tag{5.2}$$

where $i = 1, 2, \ldots, M$. Setting $a_u = [a_{u_1}, a_{u_2}, \ldots, a_{u_M}]^T$ the system of equations for the $a_u$'s

https://doi.org/10.1017/S095679251800027X Published online by Cambridge University Press

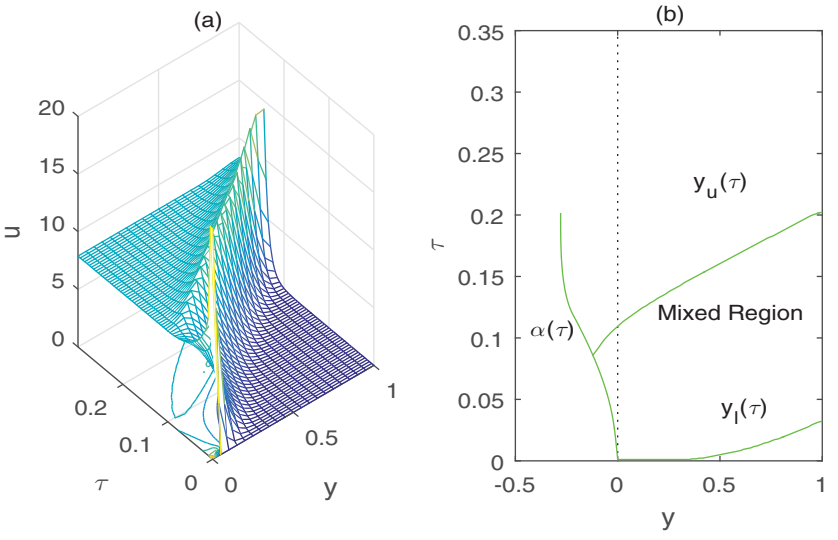


FIGURE 6. Numerical solution of the system (3.13). In (a) the variable $u$ is plotted against space and time and in (b) the moving boundaries, indicating when the corrosion is complete in the case of having an initial calcite element in the form of a square.

takes the form

$$B_l \dot{a}(\tau) = -\frac{1}{(1+\alpha(\tau))^2} B_r(\tau) a(\tau) - \frac{\dot{\alpha}(\tau)}{1+\alpha(\tau)} C a(\tau) + b_u(\tau).$$

The matrices $B_l := \left(\int_0^1 \psi_j(r)\,\psi_i(r)\,dr\right)$, $B_r := \left(\int_0^1 D(r,\tau)\psi_j'(r)\,\psi_i'(r)\,dr\right)$ and $C := \left(\int_0^1 (1-r)\psi_j'(r)\,\psi_i(r)\,dr\right)$ have the standard form in this case (e.g., see [22, 23]) and $b_u$, is the array coming from the last term in equation (5.2).

For the resulting system of ODE's we apply an implicit scheme and take

$$\left[B_l + \delta\tau \frac{1}{(1+\alpha(\tau_n))^2} B_r(\tau_n) + \delta\tau \frac{\dot{\alpha}(\tau_n)}{1+\alpha(\tau_n)} C - \delta\tau \bar{b}_u(\tau_n)\right] a_u^{n+1} = B_l a_u^n. \tag{5.3}$$

Some extra care is needed for the evaluation of $\alpha^{n+1} \simeq \alpha(\tau_{n+1})$ and of $\dot{\alpha}(\tau_{n+1}) \simeq (\alpha^{n+1} - \alpha^n)/\delta\tau$. We have that $\alpha(\tau) = \Phi(\tau)/\left(\frac{\gamma_a}{1/(1-\phi_c)+\gamma_a} - \Phi(\tau)\right)$ and that

$$\dot{\alpha}(\tau) = \frac{\frac{\gamma_a}{1/(1-\phi_c)+\gamma_a}\dot{\Phi}(\tau)}{\left(\frac{\gamma_a}{1/(1-\phi_c)+\gamma_a} - \Phi(\tau)\right)^2}, \quad \dot{\Phi}(\tau) = \frac{1}{\phi_g - \phi_c}\frac{d}{d\tau}\int_0^1 \frac{4\phi_c + \gamma_v\,(A(r,\tau) - A(r,0))}{4 + \gamma_a/(1+\gamma_a)\,(A(r,\tau) - A(r,0))} dr.$$

Then, we use the approximation $\frac{d}{d\tau}\Phi(\tau_n) \simeq (\Phi(\tau_n) - \Phi(\tau_{n-1}))/\delta\tau$.

In Figure 6 the system of equations (3.13) is solved numerically for the case that the initial shape of the calcite core is a square. In (a) $u$ is plotted against space and time. In (b) the moving boundaries, $y_l(\tau)$ and $y_u(\tau)$, given by the conditions: $\max\{\tau : A(y_l(\tau),\tau) = 4 - (2L_0)^2\}$ and $\min\{\tau : A(y_u(\tau),\tau) = 4(1+\gamma_a L_0^2)\}$, respectively, are plotted against

https://doi.org/10.1017/S095679251800027X Published online by Cambridge University Press

time (in the vertical axes) together with $\alpha(\tau)$. The values of the parameters used in these simulations are for $M = 61$, $T = .8$, $\epsilon = 1$, $\gamma_m = 1$, $\rho_c = 2.71\text{gr/cm}^3$, $\rho_g = 2.31\text{gr/cm}^3$, $\rho_m = 0.7352$ $\phi_c = 0.05$, $\phi_g = 0.15$, $\delta\tau = .8 \cdot \delta y^2$. The area between $y_l$, $y_u$ and $\alpha(\tau)$ specifies the region where the corrosion process is taking place and pure calcite and gypsum coexist in a microscopic scale.

### 5.1 Application for the case of a limestone monument corrosion

In such a case the reaction (2.2) applies. We proceed with the modelling approach described in [24].

We describe briefly the model by focusing in the minor modification needed to add in the equations already presented. According to the reaction (2.2) we have that the the molar concentration of $SO_4^{2-}$, $u$ satisfies the diffusion equation in the pores of the material

$$\epsilon_1 u_\tau = \Delta u. \tag{5.4}$$

We also have diffusion of water of dimensionless concentration $v = v(y, \tau)$ in the same domain and

$$\epsilon_2 v_\tau = \Delta v. \tag{5.5}$$

The motion of the boundary, the inner surface of the pore, is given by the standard kinetic condition expressing the fact that *Speed of the moving boundary* $\times$ *Calcium carbonate concentration* $\propto$ *Rate of reaction*. In our case and by taking into account the Law of mass action we have that the rate of reaction should have the form

$$R(y, \tau) = g(v) u v^2.$$

The function $g$ models the fact that the reaction takes its full speed when the water concentration is larger than an upper threshold $v_u$ and it does not occur at all when the concentration is lower than a lower threshold $v_l$. Between $v_l$ and $v_u$, we have to account for the fact that calcium carbonate inside the pores is covered just by water droplets and not of a water film and thus reaction takes place but not in its full speed. Such a function should have the form $g(v) = \frac{\min(\max(v, v_l), v_u) - v_l}{v_u - v_l}$ [24]. Thus, at the boundary $\Gamma_M$ the kinetic condition for the speed of the moving boundary $\mathsf{V}$ should be

$$\mathsf{V} = R(y, \tau), \quad y \in \Gamma_M. \tag{5.6}$$

Furthermore, the flux of $u$ arriving at the interface is consumed by the chemical reaction transforming concrete into gypsum. In addition, we may have transport of the residual reactant due to the motion of the boundary and thus the boundary condition at the interface of the corroded–uncorroded material, given that $\mathsf{V} = R(y, \tau)$ will be

$$\gamma_1 \frac{\partial u}{\partial n} = \mathsf{V} + \beta_1 \mathsf{V} u, \quad y \in \Gamma_M, \tag{5.7}$$

where $n$ is the outward normal vector at a point of the moving boundary $\Gamma_M$ and for

https://doi.org/10.1017/S095679251800027X Published online by Cambridge University Press

$\gamma = \gamma_u \frac{1}{\delta}$. The same should apply for the water concentration $v$ and get

$$\gamma_2 \frac{\partial v}{\partial n} = 2\mathsf{V} + \beta_2 \mathsf{V} v, \quad y \in \Gamma_M. \tag{5.8}$$

These equations apply in the porous net inside the material in $\Gamma_M$. Moreover, we consider exactly the same geometry and setting as the one described in Section 2. In the cell symmetry conditions should be applied for the variable $u$ and $v$ in the following form:

$$n \cdot \nabla u|_{\partial\Omega} = 0, \quad n \cdot \nabla v|_{\partial\Omega} = 0 \quad y \in \Gamma_e. \tag{5.9}$$

The expansion of the cell boundary is given again by :

$$\mathsf{V}_e = \frac{\partial}{\partial \tau} \left( \sqrt{|\Omega(0)| + \gamma_a A_g(\tau)} \right), \quad y \in \Gamma_e. \tag{5.10}$$

As we can see the additions in the basic model of Section 3 is that we consider also diffusion of the water and an extra equation for it, together with the specific form of the reaction term $R = R(u, v)$. Also there is no production of $u$ inside the material, that is $f \simeq f_0 = 0$ and transport of the residual reactant gives an extra term in the boundary conditions at $\Gamma_M$. The homogenization analysis can be carried out in exactly the same way and finally we can obtain the full system of equations to be solved. Namely, for $\epsilon_i, \beta_i, \gamma_i$, $i = 1, 2$, dimensionless constants [24], the equation for $u$ is

$$\epsilon_1 u_\tau - D(y,\tau) u_{yy} = -\frac{1}{\gamma_u} R(u,w)(1 + \beta_1 u) \frac{L(y,\tau)}{A(y,\tau)}, \quad -\alpha(\tau) < y < 1, \quad \tau \geqslant 0 \tag{5.11a}$$

$$u(-\alpha, \tau) = \frac{1}{\phi(-\alpha,\tau)}, \quad u_y(1,\tau) + \frac{\phi_y(1,\tau)}{\phi(1,\tau)} u(1,\tau) = 0, \tag{5.11b}$$

$$u(y,0) = u_a(y), \tag{5.11c}$$

while the diffusion equation for the water concentration $v$ has the form,

$$\epsilon_2 v_\tau - D(y,\tau) v_{yy} = -\frac{1}{\gamma_w} R(u,v)(2 + \beta_2 v) \frac{L(y,\tau)}{A(y,\tau)}, \quad -\alpha(\tau) < y < 1, \quad \tau \geqslant 0, \tag{5.12a}$$

$$v(-\alpha, \tau) = \frac{1}{\phi(-\alpha,\tau)}, \quad v_y(1,\tau) + \frac{\phi_y(1,\tau)}{\phi(1,\tau)} v(1,\tau) = 0, \tag{5.12b}$$

$$v(y,0) = v_a(y), \tag{5.12c}$$

together with the equation for the motion of the inner boundary, (3.13*d*), (3.13*e*), but with $R = R(u, v)$, as already defined, instead of $R = R(u)$, and the equations for the motion of the outer boundary (3.13*f*), (3.13*g*). In addition, $L$ and $A$ are determined by equation (3.13*h*), the porosity $\phi$ by (3.13*i*), the expansion of the macroscopic outer boundary by (3.13*j*), the variation of the diffusion coefficient by (3.13*k*), while the cell problems are given by equations (3.13*l*) and (3.13*m*).

The rest of the analysis of Section 3 can be easily adjusted to this case. The form of $\Gamma_e$ will be given in the same way. Additionally, the problem has to be transformed to a fixed domain and the left hand side of equations (5.11*a*), (5.12*a*) takes a form similar to the left hand side of equation (4.6).

We use values for the parameters taken by [7, 24] and we have $\epsilon_1 = 1.01 \cdot 10^{-12}$, $\epsilon_2 = 6.9964 \cdot 10^{-13}$, $\gamma_u = 5.98$, $\gamma_w = 1.2685 \cdot 10^{13}$, $\beta_1 = 5.053 \cdot 10^{-12}$ and $\beta_2 = 6.1131 \cdot 10^{-6}$, $\gamma_a = 0.3276$.

https://doi.org/10.1017/S095679251800027X Published online by Cambridge University Press

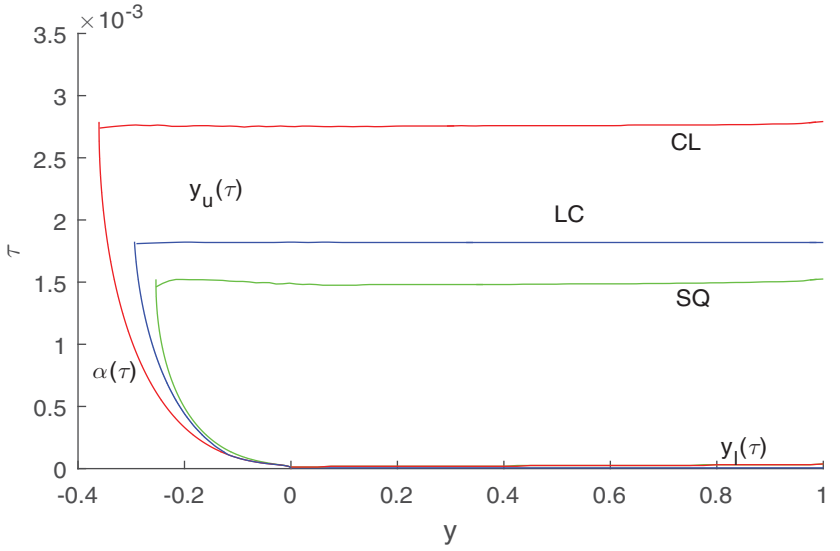


FIGURE 7. A simulation of the corrosion process for the case that we have equations (5.14) and (5.13) in place of (5.11*a*) and (5.12*a*) together with the rest of the equations of the system (3.13), for small $\epsilon_2$ and $1/\gamma_w$. The simulations are done in the case that we have in the microgeometry, (a) a square shaped core (SQ, green line), (b) a circle shaped calcite core (CL, red line) and (c) a Lame curve shaped core (LC, blue line).

Therefore, the water diffusion is very fast compared with the reaction progress. Thus, $v_{yy} \simeq 0$ for $\epsilon_2, 1/\gamma_w \ll 1$. For a constant concentration at the boundary $y = 0$, $v\phi = 1$ and $(v\phi)_y = 0$, at the point $y = 1$, and as far as $D(y,\tau) = O(1)$, $v$ is approximated by

$$v = \frac{1}{\phi(0,\tau)}\left[1 - \frac{\phi_y(1,\tau)}{\phi(1,\tau) + \phi_y(1,\tau)}y\right]. \tag{5.13}$$

Moreover, the equation for $u$, given that $\epsilon_1, \beta_1 \ll 1$, is approximated by

$$D(y,\tau)u_{yy} = \frac{1}{\gamma_u}g(v)uv^2\frac{L(y,\tau)}{A(y,\tau)}, \quad -\alpha(\tau) < y < 1, \quad \tau \geqslant 0. \tag{5.14}$$

Therefore, the quasi-steady approximation is valid for the system. For this case a simulation has been done in Figure 7 where the boundaries $y_u$ and $y_l$ are plotted against time and $S_a$ is taken to be (a) a square, (b) a circle, (c) a Lame curve. We can see that due to the fact that diffusion is fast a layer of thickness $y = 1$ ($x = l = .012$ cm), instantly becomes partly corroded, that is $y_l$ is placed very close at the $\tau = 0$ line, while this layer is fully corroded at about 0.0025 time units for a circular calcite core or at about $t = 0.0025 \times t_0 \simeq 1$ month for the timescale $t_0$ used. Corrosion is faster in the case of a Lame curve–geometry and even faster for square cell geometry The effect of the microgeometry in the process is apparent here.

https://doi.org/10.1017/S095679251800027X Published online by Cambridge University Press

### 5.2 Application for the case of sewers pipes corrosion

In the case of sewers pipes corrosion we have that $H_2S$, which is produced inside the pipes diffuses inside the pores of the pipe wall from its inner surface and through in it. Then, inside the pores of the pipe wall we have $H_2S$ in the gaseous phase with dimensionless concentration $v_g$, $H_2S$ in the liquid phase and of dimensionless concentration $v_l$, coexisting. These are exchanged between gaseous and liquid phase. Moreover, the liquid $H_2S$ due to bioconversion is transformed to $SO_4^{2-}$, of dimensional concentration $u$, which in tern reacts with the calcite of the inner wall of the pore producing gypsum $CaSO_4 \cdot 2H_2O$. The latter process, which actually is the cause of the corrosion, is described by the reaction (2.1).

The equations in dimensionless form expressing the evolution of the concentrations inside the pores of the material, see [5, 22, 23], are

$$\epsilon_1 \frac{\partial v_g}{\partial \tau} = \frac{\partial^2 v_g}{\partial y^2} - \mu_1 \left(\beta_1 v_g - v_l\right), \tag{5.15a}$$

$$\epsilon_2 \frac{\partial v_l}{\partial \tau} = \frac{\partial^2 v_l}{\partial y^2} + \mu_2 \left(\beta_1 v_g - v_l\right) - \beta_2 v_l, \tag{5.15b}$$

$$\epsilon_3 \frac{\partial u}{\partial \tau} = \frac{\partial^2 u}{\partial y^2} + \beta_3 v_l, \tag{5.15c}$$

with $\epsilon_i$, $\beta_i$, $i = 1, 2, 3$, $\mu_1$, $\mu_2$ dimensionless constants [22]. The motion of the moving boundary inside the pore of the material is given by (3.13*d*), (3.13*e*), but with

$$R(y, \tau) = u, \quad y \in \Gamma_M. \tag{5.16}$$

After applying the averaging process in the same way as before and having in mind that for $v_g$ and $v_l$ Neumann conditions hold for the moving boundary $\Gamma_c$, we obtain for the macroscopic scale

$$\epsilon_1 \frac{\partial v_g}{\partial \tau} = D(y, \tau) \frac{\partial^2 v_g}{\partial y^2} - \mu_1 \left(\beta_1 v_g - v_l\right), \tag{5.17a}$$

$$\epsilon_2 \frac{\partial v_l}{\partial \tau} = D(y, \tau) \frac{\partial^2 v_l}{\partial y^2} + \mu_2 \left(\beta_1 v_g - v_l\right) - \beta_2 v_l, \tag{5.17b}$$

$$\epsilon_3 \frac{\partial u}{\partial \tau} = D(y, \tau) \frac{\partial^2 u}{\partial y^2} + \beta_3 v_l + F(u), \tag{5.17c}$$

for $F(u) = -\frac{1}{\gamma_u} R(u) \frac{L(y,\tau)}{A(y,\tau)}$ as in equation (3.13*a*), while the same equations (3.13*d*)–(3.13*l*) apply as before. Note also that here in equation (5.17*c*) the term $\beta_3 v_l$ plays the role of $f$ in equation (3.13*a*). This set of equations can be completed with appropriate boundary and initial conditions of the form (3.13*b*) and (3.13*c*) for all concentrations $v_g$, $v_l$, $u$.

In the case that we evaluate the dimensionless constants with specific values of the parameters (cf. [5, 22]) we may obtain small values for $\epsilon$ and large values for $\mu$. More specifically, we have $\epsilon_1, \epsilon_2, \epsilon_3 \ll 1$ and $\mu_1, \mu_2 \gg 1$, $\beta_1 = 1$, giving $v_g \sim v_l$ and allowing us to apply again a quasi steady approximation. In such a case the model equations to be

https://doi.org/10.1017/S095679251800027X Published online by Cambridge University Press

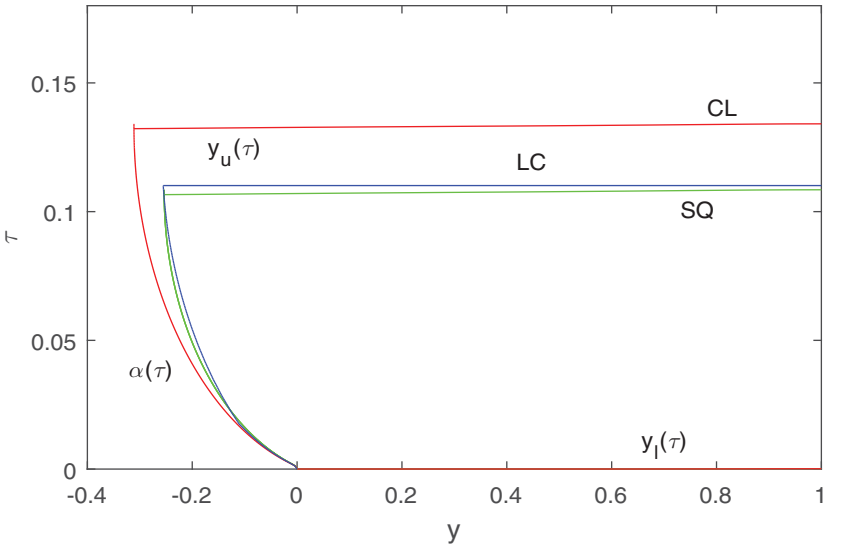


FIGURE 8. A simulation of the corrosion process for the case that we have equations (5.18*a*) and (5.18*b*) in place of (5.17*b*) and (5.17*c*) together with the rest of the equations in the system (5.17), for small $\epsilon_2, \epsilon_3$ and a square (green line), circular (red line) or Lame curve (blue line) shaped calcite core in the microgeometry. In general there is visible difference in the final result regarding the microstructure consideration. We observe faster corrosion in the case of square cell and slower in the case of a cyclic cell. For a cell shaped as a lame curve the behaviour is intermediate.

solved become

$$D(y,\tau)\frac{\partial^2 v_l}{\partial y^2} - \beta_2 v_l = 0, \tag{5.18a}$$

$$D(y,\tau)\frac{\partial^2 u}{\partial y^2} + \beta_3 v_l + F(u) = 0. \tag{5.18b}$$

A simulation is presented in Figure 8. We notice some small variations between the boundaries with respect to the considered microstructure geometry (square, circle or Lame curve shaped calcite core). The corrosion is faster in the case of the square-cell geometry. The effect of diffusion is fast, the material becomes immediately everywhere partly corroded and fully corroded simultaneously at a later time. The material is fully transformed, for example, for the case of circle, at about 0.1328 time units, which in dimensional terms, gives that a layer of 13 cm is fully corroded after 22.67 years.

## 6 Discussion

The major issue in the present paper is to expand an existing model, describing calcium carbonate corrosion and also addressing the formation of a mixed (mushy) region during this process. The modelling expansions include the phenomenon of volume expansion coming from the difference in the density of calcite and gypsum, as well as the variation of the diffusion, resulting from the shape evolution of the calcite part inside a pore. Homogenization method is applied to derive a set of macroscopic equations which can be solved numerically.

https://doi.org/10.1017/S095679251800027X Published online by Cambridge University Press

In some cases, the complete set of the resulting equations can be simplified so as to diminish the numerical complications. For the same reason in the micro-scale only two-dimensional geometry is considered. Some simulations for various cases are presented.

An important aspect to be addressed in a future work should be the study of existence, uniqueness and asymptotic properties of the solution of the macroscopic model derived in this work.

Of course, further extensions of this work, regarding the modelling approach and the derivation of macroscopic equations, should include three-dimensional micro-scale geometry. Another aspect avoided at present, and in possible future research, is to include in the model the stress forces between the cells and due to volume expansion. Also additional simulations for different macroscopic geometries could be another interesting aspect. Moreover this model can be adjusted to other similar phenomena where we have corrosion in a porous media.

## Acknowledgements

The author wants to express his gratitude to the anonymous reviewers and especially reviewer # 1 for his valuable and important remarks regarding various aspects of this work.

## References

[1] Ali, G., Furuholt, V., Natalini, R. & Torcicollo, I. (2007) A mathematical model of sulphite chemical aggression of limestones with high permeability. Part I. Modeling and qualitative analysis. *Transp. Porous Media* **69**, 109–122.

[2] Ali, G., Furuholt, V., Natalini, R. & Torcicollo, I. (2007) A mathematical model of sulphite chemical aggression of limestones with high permeability. Part II: numerical approximation. *Transp. Porous Media* **69**, 175–188.

[3] Aregba-Driollet, D., Diele, F. & Natalini, R. (2004) A mathematical model for the sulphur dioxide aggression to calcium carbonate stones: numerical approximation and asymptotic analysis. *SIAM J. Appl. Math.* **64**, 1636–1667.

[4] Beven, K. & Feyen, J. (2002) The future of distributed modelling. *Hydrol. Process.* **16**, 169–172. doi:10.1002/hyp.325.

[5] Böhm, M., Devinny, J., Jahani, F. & Rosen, G. (1998) On a moving-boundary system modelling corrosion in sewer pipes. *Appl. Math. Comput.* **92**, 247–269.

[6] Bohm, M., Devinny, J. S., Jahani, F., Mansfeld, F. B., Rosen, I. G. & Wang, C. (1999) A moving boundary diffusion model for the corrosion of concrete wastewater systems: simulation and experimental validation. In*: Proceedings of the American Control Conference,* June 1999, San Diego, California, pp. 1739–1743.

[7] Clareli, F., Fasano, A. & Natalini, R. (2008) Mathematics and monument conservation: free boundary models of marble sulfation. *SIAM J. Appl. Math.* **69**(1), 149–168.

[8] Fasano, A. & Natalini, R. (2006) Lost beauties of the acropolis: what mathematics can say. *SIAM News* **39**(6), July/August 2006.

[9] Fatima, T., Arab, N., Zemskov, E. P. & Muntean, A. (2011) Homogenization of a reaction–diffusion system modeling sulfate corrosion of concrete in locally periodic perforated domains. *J. Eng. Math.* **39**(2–3), 261–276.

[10] Fatima, T. & Muntean, A. (2014) Sulfate attack in sewer pipes: derivation of a concrete corrosion model via two-scale convergence. *Nonlinear Anal.: Real World Appl.*, **15**, 326–344, doi: 10.1016/j.nonrwa.2012.01.019.
[11] Gregg, S. J. & Sing, K. S. W. (1982) *Adsorption, Surface Area and Porosity*, Academic Press, London.
[12] Guarguaglini, F. R. & Natalini, R. (2007) Fast reaction limit and large time behavior of solutions to a nonlinear model of sulphation phenomena. *Commun. Partial Differ. Equ.* **32**, 163–189.
[13] Guarguaglini, F. R. & Natalini, R. (2005) Global existence of solutions to a nonlinear model of sulphation phenomena in calcium carbonate stones. *Nonlinear Anal.: Real World Appl.* **6**, 477–494.
[14] Hinch, E. J. (1991) *Perturbation Methods*, Cambridge University Press, Cambridge.
[15] Howison, S., Lacey, A., Movack, A. & Ockendon, J. (2003) *Applied Partial Differential Equations*, Oxford University Press, Oxford.
[16] Jaklic, A., Leonardis, A. & Solina, F. (2000) Segmentation and recovery of superquadrics. In: *Computational Imaging and Vision*, Vol. 20, Kluwer, Dordrecth.
[17] Lacey, A. A. & Herraiz, L. A. (2002) Macroscopic models for melting derived from averaging microscopic Stefan problems I: simple geometries with kinetic undercooling or surface tension. *Euro. J. Appl. Math.* **11**, 153–169.
[18] Lacey, A. A. & Herraiz, L. A. (2002) Macroscopic models for melting derived from averaging microscopic Stefan problems II: effect of varying geometry and composition. *Euro. J. Appl. Math.* **13**, 261–282.
[19] Maragos, P. & Butt, M. A. (2000) Curve evolution, differential morphology, and distance transforms applied to multiscale and eikonal problems. *Funtamenta Informatica* **41**, 91–129.
[20] Muntean, A. & Böhm, M. (2009) A moving-boundary problem for concrete carbonation: global existence and uniqueness of weak solutions. *J. Math. Anal. Appl.* **350**(1), 234–251.
[21] Muntean, A. & Chalupecky, V. (2011) Homogenization method and multiscale modeling. In: *Lecture Notes of the Institte for Mathematics for Industry*, Vol. 34, Kyushu University, Fukuoka, Japan.
[22] Nikolopoulos, C. V. (2010) A mushy region in concrete corrosion. *Appl. Math. Model.* **34**, 4012–4030.
[23] Nikolopoulos, C. V. (2015) Macroscopic models for a mushy region in concrete corrosion. *J. Eng. Math.* **91**, 143–163.
[24] Nikolopoulos, C. V. (2014) Mathematical modelling of a mushy region formation during sulfation of calcium carbonate. *Netw. Heterog. Media* **9**(4), 635–654.
[25] Osher, S. & Sethian, J. A. (1988) Fronts propagating with curvature-dependent speed: algorithms based on Hamilton–Jacobi formulations. *J. Comput. Phys.* **79**(1), 12–49.
[26] Persson, P. O. & Strang, G. (1988) A simple mesh generator in MATLAB. *SIAM Rev.* **46**(2), 329–345.
[27] Schröder, J. (2014) A numerical two-scale homogenization scheme: the FE2-method. In: J. Schröder & K. Hackl (editors), *Plasticity and Beyond. CISM International Centre for Mechanical Sciences*, Vol. 550, Springer, Vienna.